FUTRELL, ANDREW BRYANT, M.A. Detecting the Presence of an Urban Heat Island at Three Major North Carolina Airports; and Locating Climatologically Appropriate Sites for a Piedmont Triad Weather Station (2012)
Directed by Dr. Jay Lennartson. 79 pp.

Given the urbanization that has taken place adjacent to PTIA it is likely that the Piedmont Triad International Airport's (PTIA) KGSO Automated Surface Observing System (ASOS) weather station has been impacted by an urban heat island (UHI) effect. This local-scale phenomenon has influenced and will continue to influence meteorological observations at the PTIA weather station. This research will construct a raster data model to locate sites without contamination of an UHI. The new weather station site will be a suitable alternative to PTIA.

To determine if an UHI is impacting PTIA, the average monthly minimum and maximum temperatures were analyzed using three separate statistical procedures. First, a deviation test was used to find any decoupling of average monthly minimum from average monthly maximum temperatures. Second, a Student's *t*-Test checked for significant difference for any decouplings found using the deviation statistic. Lastly, a correlation statistic is applied to test if a positive correlation exists between average monthly minimum temperatures with a running total of commercial/industrial land-use in close proximity to each airport. The above procedures determined that KGSO has been influenced by an urban heat island effect.

The second part of this study employed a raster data model to locate 'ideal' sites for KGSO, using criteria set by the World Meteorological Organization (Appendix F). In particular factors analyzed were land-use, elevation, slope, hallows, water, and

impervious surface. The raster date model can be used to find ideal alternatives for other heat island influenced weather stations.

DETECTING THE PRESENCE OF AN URBAN HEAT ISLAND AT THREE MAJOR NORTH CAROLINA AIRPORTS; AND LOCATING CLIMATOLOGICALLY APPROPRIATE SITES FOR A PIEDMONT TRIAD WEATHER STATION

by

Andrew Bryant Futrell

A Thesis Submitted to
the Faculty of The Graduate School at
The University of North Carolina at Greensboro
in Partial Fulfillment
of the Requirements for the Degree
Master of Arts

Greensboro
2012

Approved by

Dr. Jay Lennartson
Committee Chair

APPROVAL PAGE

This thesis has been approved by the following committee of the Faculty of The Graduate School at The University of North Carolina at Greensboro.

Committee Chair Dr. Jay Lennartson

Committee Member Dr. Zhi-Jun Liu

Committee Member Dr. Keith Debbage

03/30/2012
Date of Acceptance by Committee

03/30/2012
Date of Final Oral Examination

ACKNOWLEDGEMENTS

I first want to thank my committee chair: Dr. Jay Lennartson, for information, organization, and guidance on my research. Thanks to Dr. Zhi-Jun Liu, for explaining deviations and statistical approaches to research. Dr. Keith Debbage, for learning about urban form and development, land-use, and planning applications. Dr. Rick Bunch, for teaching me how to create a raster data model, acquiring raster data, and using GIS tools. Dr. Bill Tyminski, for the advice to use a Student's *t*-Test in my research. Mr. Terry Hudgins (Raleigh NWS) and Dr. Ryan Boyles (NC State Climate Office), for their information on the station history of KGSO. Mr. Grady Bare, for his information on county owned land used by the Greensboro Aeromodelers. Mr. Nicholas Leonard, for his knowledge on landscape photography techniques. I mostly would like to thank my parents, Tom and Esther, for all their support of my continuing education. I would not be where I am today without their assistance.

TABLE OF CONTENTS

LIST OF TABLES

Page

LIST OF FIGURES

CHAPTER I

INTRODUCTION

The Problem

Because of the considerable commercial development that has occurred in close proximity to the Piedmont Triad International Airport PTIA[1] over the last two decades, it is likely that an urban heat island (UHI) has been affecting, among other meteorological parameters, temperatures observed and recorded at the National Weather Service's (NWS) first order weather station, located at the airport.

As cursory evidence for this hypothesis, a simple statistical comparison of the 1971-2000 Climate Normals[2] at PTIA with those from 1981– 2010, reveals that the mean minimum temperature increased 1.3 degrees Fahrenheit compared to a 0.6 degree Fahrenheit increase for the mean maximum temperature (Appendix A). This finding is consistent with other investigations of the influence of an UHI on temperature which have shown that an UHI causes warmer minimum temperatures at night, while maximum temperatures remain steady or decrease slightly (e.g., Zhang, Sato, Izumi, Aramaki, & Hanaki, 2008; Sarrat, Lemonsu, Masson, & Guedalia, 2006).

It is critical to climate scientists studying climate-related problems, such as global warming, that they have access to long-term, continuous, and unbiased temperature records at climate stations in the United States, and around the globe. When temperature

[1] PTIA is located in Greensboro, NC
[2] Climate Normals for Greensboro (KGSO)

records, such as those at PTIA have been corrupted by anthropogenic influences at the local-scale, e.g., an UHI, the study of climate change is made much more challenging. With this in mind, the primary goal of this researcher is to determine conclusively whether an UHI is present in the environs of PTIA; and if present how it has been influencing temperatures measured and recorded by the NWS at PTIA—because understanding these factors can allow for a better understanding of how the UHI influences meteorological data measured at weather stations, like that at PTIA (Han & Baik, 2008; Bejaran & Camilloni, 2003).

Development of an UHI and its Relationship to PTIA

UHI Development

An UHI exists when a temperature gradient is observed between urban and rural areas (Memon, Leung, & Liu, 2009). This phenomenon is commonly found in urbanized areas worldwide and has impacts on local climate. Changes in surface features and anthropogenic heat are the primary causes of an UHI (Han & Baik, 2008; Khan & Simpson, 2001). When natural vegetation is altered or removed on a large scale it changes the surface energy budget (Atkinsin, 2003). Typical landscapes in an urban area include asphalt surfaces, buildings, structures, and little vegetation. Impervious surfaces contain a high specific heat relative to natural vegetation (Memon et al., 2009). During diurnal hours, larger amounts of shortwave energy are stored in these bodies (Memon et al., 2009). At night this extra energy is emitted in the infrared spectrum. This offsets radiational cooling in an urbanized area. An UHI can impact an area during day or night, but has the largest impact on minimum temperature (Atkinsin, 2003).

Synoptic-Scale Influences on PTIA's UHI

Synoptic weather patterns, air masses, and prevailing winds can also have an impact on an UHI (Khaikine, Kuznetsova, Kadygrov, & Miller, 2006). The UHI has the greatest influence during summer months for mid-latitude locations (Kolokotsa, Psomas, & Karapidakis, 2009). In the Piedmont Triad (and throughout the Southeast U.S.) a synoptic-scale high pressure cell is the dominant synoptic-scale weather feature. The subsidence associated with high pressure cells reduces vertical air mixing and causes light winds at the surface (Kolokotsa et al., 2009). When vertical mixing does not occur, additional heat produced at the surface remains trapped. This additional heat is what causes the urban heat island. Impervious surfaces store heat during daytime hours when air is stagnant and the sun angle is high (Kolokotsa et al., 2009). The subsidence and high sun angle during the summer is when the UHI effect is expected to be strongest at PTIA.

An UHI's Impact on Local Forecasting

The UHI effect can produce minimum temperatures significantly warmer than minimum temperatures on the periphery of urban regions. The difference becomes significant when an urban/rural temperature gradient is repeatedly observed. For example, a frost or freeze can occur outside the influence of the UHI in rural areas, while the urban areas do not frost or freeze. This can impact forecast used for agricultural purposes outside the area impacted by UHI.

How Urban Form Influences an UHI

The size of an urbanized region has a greater impact than the density in UHI formation (Nichol, Fung, Lam, & Wong, 2009). KGSO is surrounded by widespread low density development (urban sprawl). This type of development has the greatest influence in UHI formation. Prior research has shown commercial and industrial land-use change can impact air temperature on a regional scale (Kolokotsa et al., 2009). Wind speed and direction can also influence the size and formation of an UHI (Kolokotsa et al., 2009). A study conducted in Atlanta, GA used a linear regression model to calculate and predict impervious surface coverage (Lee & French, 2009). This study subdivided impervious surfaces into two categories: industrial/commercial development and residential development (Lee & French, 2009). These two categories were further divided into light or dark materials (Lee & French, 2009). Dark materials have a lower albedo and absorb more shortwave radiation (Lee & French, 2009). Industrial and commercial parcels on average have more impervious surface than residential land-use. As a result this produces a lower average albedo which enhances UHI formation. The predominant development around PTIA has been commercial/industrial land-use. This land-use will be analyzed for its connection to the formation of the UHI at PTIA.

The Rule of Urban Planning in Mitigating an UHI

Due to an UHI's negative impacts on local climate, urban and regional planners have explored different methods to mitigate UHI formation. Studies have attempted to reverse UHI contributing factors through rearranging parcels to have additional shading (Stone & Norman, 2006). Urban climate zoning can be exercised to reduce or prevent an existing UHI from getting worse (Yang, Lau, & Qian, 2011). This can be accomplished by planting trees (Yang et al., 2011), using reflective roofs (Gober et al., 2010), using glazing windows (Smith & Levermore, 2008), building parks (C. Chang, Li, & S. Chang, 2007), creating watered landscapes (Coutts, Beringer, & Tapper, 2010), increasing surface albedo (Synnefa, Dandou, Santamouris, & Tombrou, 2008), constructing roads with water-holding pavement (Nakayama & Fujita, 2010), or converting asphalt parking lots to grass lots (Takebayashi & Moriyama, 2009). For KGSO, these UHI mitigation techniques are costly and complicated to implement. The area of interest is large, fragmented, and jurisdictionally divided. It would be difficult to enforce these planning practices. As a result, another option (discussed below) will be explored in this study.

Development of a GIS Raster Data Model

Since the UHI cannot be mitigated near PTIA, the only other viable option is to relocate the PTIA weather station. A GIS model using raster data will be used to find locations not impacted by the UHI effect at KGSO. The objective here is to find an 'ideal' site for a weather station near PTIA. An 'ideal' site would provide climate readings similar to those at KGSO without the influence of the urban heat island.

Ultimately the goal of this model portion of the research is to develop a method that is not limited to just KGSO, but can also serve as a template to locate alternate sites for other weather stations impacted by an UHI.

CHAPTER II

STUDY AREAS

This research will analyze temperature data at weather stations at KGSO, KCLT, and KRDU to see if an UHI exists at any of the three sites. The geographic locations of these airports are either west or northwest of a large city. All three stations are Automated Surface Observing Systems (ASOS), first order climate stations, so data quality is exceptional (Guide to Meteorological Instruments and Methods of Observation [WMO], 2006). These locations are large, flat, and open areas. The openness allows for wind fetch and atmospheric mixing in all directions (WMO, 2006). As a result, observed temperatures are representative of their respective regions (WMO, 2006). KGSO, KRDU and KCLT are located in the Piedmont plateau region of North Carolina. These locations experience similar climate annually. Mid-latitude cyclones, warm/cold fronts, tropical cyclones, sub-tropical high pressure cells and summer convection all impact these locations. Precipitation totals are uniform and mean minimum and mean maximum temperatures are similar. KCLT and KRDU were chosen based on their data quality, geographic proximity, and climatic compatibility to KGSO. The urban form surrounding each site will be examined in the following paragraphs. This is important because the surrounding land-use at a weather station site can potentially impact its measurements.

KGSO (ASOS Site for Piedmont Triad International Airport)

The Piedmont Triad International Airport (PTIA) may be seen in Figure 1. This figure shows an orthoimage (aerial photograph) of the landscape surrounding the airport. Overlaid on top of the orthoimage are semi-transparent polygons. These polygons represent individual industrial or commercial land parcels. The varying colors of the polygons represent the year when the parcel was developed. The hollow yellow circle represents a 2.5 mile buffer from the center of the KGSO weather station (see red star). The 2.5 mile buffer was used because CO-OP weather stations are normally located within 2 miles of the parent weather station (National Climatic Data Center [NCDC], 2011). By looking beyond the distance recommended by the National Climatic Data Center (NCDC), it is clear the urban development extends beyond this criteria. As a result, relocating the PTIA weather station inside this area would be difficult, if not impossible, to accurately record meteorological observations. KGSO (Figure 1) has a considerable amount of industrial/commercial land-use adjacent to the periphery of the airport to the east, south, and west of the ASOS site (see red star). A total of 514 industrial/commercial parcels are seen on this map, covering 3611.7 acres of land. Three-hundred ninety of these parcels were developed since 1980. The 390 parcels account for 2631.4 acres of developed land. The ratio of the land developed since 1980 (2631.4 acres) to the total land developed (3611.7 acres), equates to 72.9% of the total commercial/industrial land-use. Linking this rapid development to the cause of the UHI effect is of interest in this study.

Before taking this study further, confirmation of station history and location must be established. Contact was made with the North Carolina State Climate Office and the Raleigh National Weather Service. They confirmed the current ASOS site for KGSO is where hand measurements were taken from 1928 to 1995 (T. Hudgins, personal communication, June 6, 2011). After 1995, major airports switched to the Automated Surface Observing System (ASOS) (WMO, 2006). Prior to the rapid development in the 1980s and 1990s, KGSO was surrounded by farmlands and forest. The southwest and northwest corners of this image are representative of the land-use near PTIA prior to the start of commercial and industrial development adjacent to PTIA in the 1980s (Figure 1).

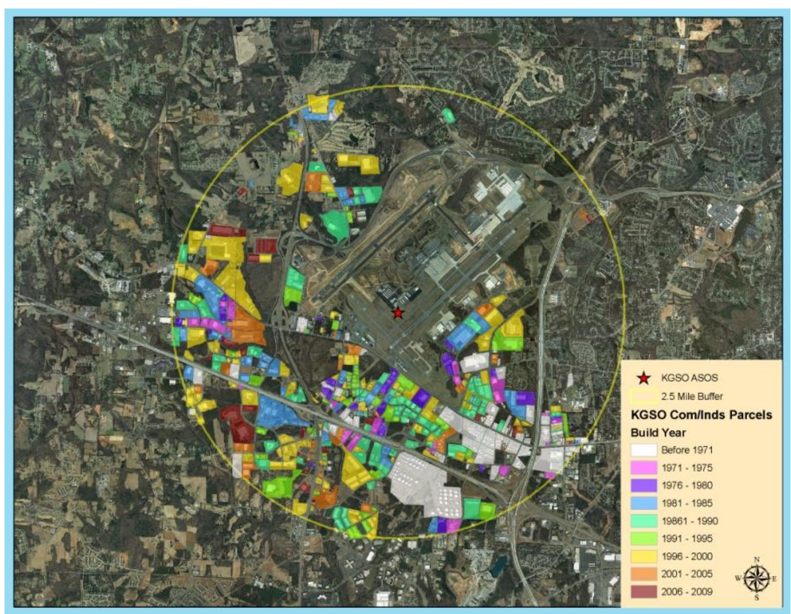

Figure 1. Piedmont Triad International Airport. 2010 North Carolina Orthoimagery for PTI Airport (NC OneMap) and Commercial/Industrial Parcels (Guilford County GIS) sorted by build year. The yellow line represents a 2.5 mile buffer to show proximity of commercial/industrial land-use to KGSO ASOS observation (red star).

KCLT (ASOS Site for Charlotte-Douglas International Airport)

The ASOS site for KCLT will now be examined (Figure 2). The same spatial scale as in the first study area was used to allow comparison between the two locations. The commercial/industrial land-use surrounding KCLT is less dense in comparison to KGSO. The urban development is isolated to the northeast, east, and southeast of KCLT (see red star). The development is not only less dense, but is also further away from the weather station site (see red star). KCLT has considerably more forested area and green space than KGSO. The vegetative land-use is larger spatially and closer to the ASOS site. A total of 274 commercial/industrial parcels are seen in Figure 2, covering 1262.3 acres of land. One-hundred forty-three of these parcels were developed since 1980. The 143 parcels account for 824.7 acres of developed land. The ratio of the land developed since 1980 (824.7 acres) to the total land developed (1262.3 acres), equates to 65.3 % of commercial/industrial land-use. The rate of development around KCLT has been slower since 1980 and the total developed land is less than the total land developed for KGSO by 2349.4 acres (3611.7 acres minus 1262.3 acres). The isolation from urban development, openness, and the abundance of green-space are good qualities for a regional weather station. Thus KCLT will serve as a climatologically appropriate weather station for this region.

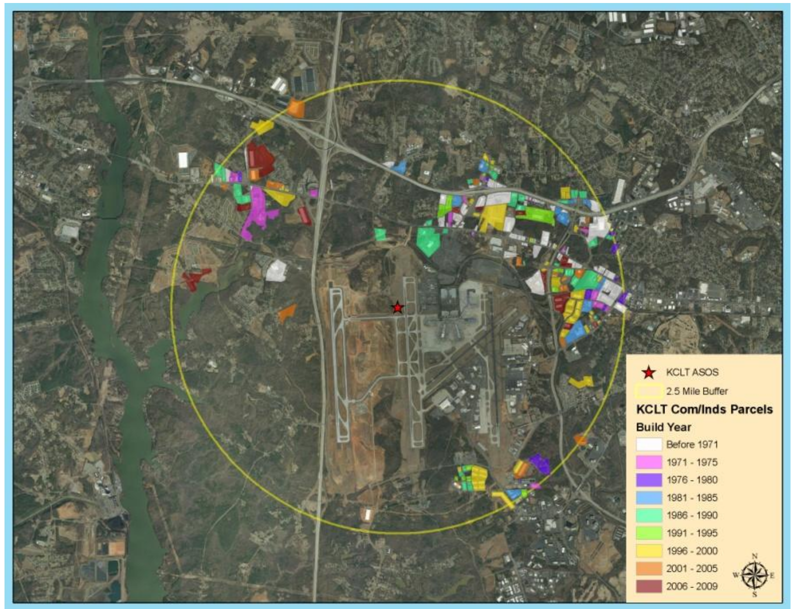

Figure 2. Charlotte-Douglas International Airport. 2010 North Carolina Orthoimagery for Charlotte-Douglas International Airport (NC OneMap) and Commercial/Industrial Parcels (Mecklenburg County GIS) sorted by build year. The yellow line represents a 2.5 mile buffer to show proximity of commercial/industrial land-use to KCLT ASOS observation (red star).

KRDU (ASOS Site for Raleigh-Durham International Airport)

The ASOS site for KRDU will now be examined (Figure 3). Visually KRDU is more similar to KCLT than KGSO. Like KCLT, KRDU has considerably more green-space than KGSO. A large portion of this green-space exists as a tree-line buffer around the periphery of Raleigh-Durham International Airport. The tree-line is a buffer because it separates KRDU from commercial/industrial development off-site from the airport. The adjacencies to William B. Umstead State Park to the south and wetlands protection to the west are the primary reasons for this buffer. This tree-line will offset waste heat from urban development along Interstate 40, Interstate 540, and U.S. 70. The pockets of development around KRDU are fragmented to the south and west and a little more concentrated to the north. Similar to KCLT, the development at KRDU is not encroaching on the perimeter of the airport. A total of 382 commercial/industrial parcels are seen in Figure 3, covering 1587.0 acres of land. Three-hundred eighteen of these parcels were developed since 1980. The 318 parcels account for 1394.9 acres of developed land. The ratio of the land developed since 1980 (1394.9 acres) to the total land developed (1587 acres), equates to 87.9% of commercial/industrial land-use. The rate of development is higher at KRDU than KCLT or KGSO; however, very little land was developed around KRDU prior to 1980. The total land developed at KRDU is lower than KGSO. KGSO has 2024.7 more developed acres of land than KRDU (3611.7 acres minus 1587.0 acres).

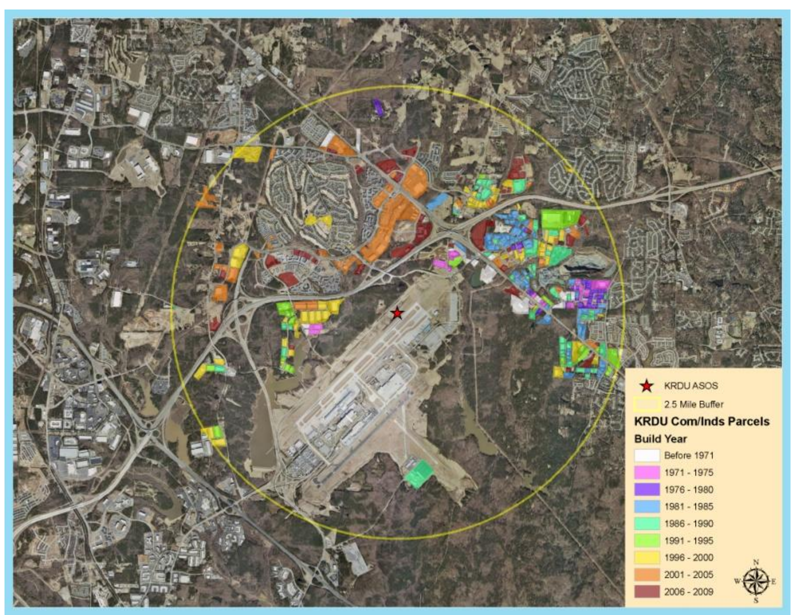

Figure 3. Raleigh-Durham International Airport. 2010 North Carolina Orthoimagery for Raleigh-Durham International Airport (NC OneMap) and Commercial/Industrial Parcels (Durham and Wake Counties GIS) sorted by build year. The yellow line represents a 2.5 mile buffer to show proximity of commercial/industrial land-use to KRDU ASOS observation (red star).

The local land records show significantly more industrial/commercial development in close proximity to KGSO compared to KCLT or KRDU. KGSO has a total of 3611.7 acres of developed commercial/industrial land-use, while KCLT has 1262.3 acres and KRDU has 1587.0 acres of commercial/industrial land developed. Combining the total industrial/commercial land-use for KCLT and KRDU equals 2849.3 acres of developed land. The total commercial/industrial land-use for KGSO (3611.7 acres) is greater than the combined total of commercial/industrial land-use for KCLT and KRDU (2849.3 acres). This higher amount of development and the spatial proximity of this new development to KGSO is the likely cause of the urban heat island effect seen in the local climate records.

CHAPTER III

PROCEDURES

Statistical Analyses Used to Determine the Presence of an UHI

This chapter will discuss three statistical methods for identifying the influence of an UHI on local climate records. Before discussing these methods, daily climate records will be analyzed for KGSO. The daily climate parameter to be analyzed is minimum temperature. This parameter was chosen because UHI has the greatest influence on minimum temperatures, therefore an UHI could inflate the number of high minimum temperatures at an affected weather station. A high minimum temperature record occurs when the minimum temperature for a particular day of the year remains higher than all other past or present minimum temperatures for that day. For example, the high minimum temperature at KGSO on July 23rd was 78 Fahrenheit (APPENDIX C). This high minimum temperature record occurred in 2005. This means all other minimum temperatures recorded on this particular day were lower than 78 Fahrenheit for KGSO.

Daily climate records are not sufficient by themselves to give statistical proof of an UHI, but they serve as evidence that an UHI at PTIA may be influencing the climate record. The station history of KGSO covers 84 years from 1928 to present. Daily climate records are normally random and evenly distributed; however, the field of high minimum temperature showed a high frequency of high minimum records in the last two decades. Most of these high minimum records occurred in the months of June, July, and

August. These months were chosen because research confirms an UHI has the greatest impact during the summer for mid-latitude regions. The month of June has a total of 30 days. Sixteen of these days recorded a record high minimum temperature since 1990 (Appendix B). The month of July has a total of 31 days. Twenty of these days recorded a record high minimum temperature since 1990 (Appendix C). The month of August also has 31 days. This month had an impressive 27 days of record high minimum temperatures since 1990 (Appendix D). Many of these records are likely associated with the land-use change adjacent to the airport. For comparison, the month of January was also analyzed for record high minimum temperatures. January has a total of 31 days. Seven of these days recorded a record high minimum temperature since 1990 (APPENDIX G). The occurrences of records for January compared to June, July, or August is considerably lower. The all-time record high minimum temperature for KGSO, 80 Fahrenheit, was set August 9th, 2007 (Appendix E). This minimum temperature occurred in an environment with few clouds, no wind, and a dew point temperature of 70 Fahrenheit (Appendix E). Both KCLT and KRDU recorded minimum temperatures of 78 Fahrenheit under similar conditions to KGSO (Appendix E). These daily records were not used in the statistical methods of this study, however; these daily records were likely aided by an UHI. The next step in this research involves data acquisition and an explanation of statistical methodologies used for UHI identification.

Climate records were obtained from the National Climatic Data Center (NCDC). In order to statistically compare KGSO, KCLT, and KRDU, the same time series must be used. It was important to determine when climate records were first kept for each station.

Climate data for KGSO began in 1928; data for KCLT began in 1939; and data for KRDU began in 1944. Since 1944 was the earliest year in which data was available for all three weather stations, a time series will analyze the period from 1944 to 2009. The two variables obtained for this study were average monthly minimum temperature (T_(avg-mly-min)) and average monthly maximum temperature (T_(avg-mly-max)). This data was collected for the months of June, July, and August for KGSO, KCLT, and KRDU. Following data acquisition there were three statistical procedures used to analyze the data for trends characteristic of an UHI. The statistical analyses used were deviation, Student's *t*-Test, and correlation.

Deviation

In statistics, deviation is a measure of difference for variables between the observed value and the mean. Deviation can be computed for interval or ratio scale variables. This study uses the variable of temperature measured in degrees Fahrenheit. Degrees Fahrenheit uses an interval scale since the zero point is arbitrary. The deviation is used to determine the magnitude of the difference of observed values with respect to the mean. A positive deviation is greater than the mean, while a negative deviation is less than the mean. The sum of all deviations is zero and conversely the average deviation is also zero. Concerning temperature, deviations can be used to show warming trends (positive deviation) and cooling trends (negative deviation).

The deviation statistic will be used to find temperature trends between T_(avg-mly-min) and T_(avg-mly-max). These two variables will be analyzed on the same graph because a deviation statistic uses the common mean of zero. The magnitude (the difference of observed value from the mean) will be examined to determine if warming and cooling periods for T_(avg-mly-min) and T_(avg-mly-max) are similar. In general, an ASOS weather site should observe similar changes in magnitude for T_(avg-mly-min) and T_(avg-mly-max). A common characteristic of an UHI is a decreased diurnal temperature range (DTR) (Easterling et al., 1997). The decrease is the result of warming minimum temperature relative to maximum temperature (Easterling, 1997). This trend is represented by a decoupling of T_(avg-mly-min) from T_(avg-mly-max) when using the deviation statistic. An UHI influenced weather observation will show T_(avg-mly-min) considerably warmer compared to T_(avg-mly-max) when using a 67 year average.

This research uses a deviation statistic to find the yearly magnitude of T_(avg-mly-min) and T_(avg-mly-max) for July (and the three-month period ($\underline{X}_s$): June, July, and August) using a 67 year average. The average was established using a time series from 1944 to 2009. To find the magnitude, the 67 year average must first be calculated. This was computed by summing the terms ($X_{1+\ldots+}$ $X_{n=67}$) and dividing by the period (*n*=67) (Equation 1). This will compute the July T_(avg-mly-min) and T_(avg-mly-max) for the 67 year period. This method will also be used to calculate the three-month T_(avg-mly-min) and T_(avg-mly-max) for June, July, and August. An additional step will require summing the T_(avg-mly-min) and T_(avg-mly-max) terms for the three-month period ($\underline{X}_s$) ($\underline{X}_1$ = June, $\underline{X}_2$ = July, and $\underline{X}_3$ = August and dividing by three (Equation 2). This will compute the T_(avg-mly-min) and T_(avg-mly-max) for the period of June, July and August.

$$\underline{X} = (X_{1+\ldots+} X_n)/n \quad (1)$$

$$\underline{X}_s = (\underline{X}_1 + \underline{X}_2 + \underline{X}_3)/3 \quad (2)$$

The next step towards calculating the deviation statistic is computing the magnitude (difference) for each year using the averages calculated in Equation 1.

For the T_(avg-mly-min) and T_(avg-mly-max) for July the difference is calculated as follows (Equation 3):

$$\ddot{\varepsilon}_i = X_i - \underline{X} \quad (3)$$

The magnitudes were also calculated for the three-month period (Equation 4) using the averages computed in Equation 2.

$$\ddot{\varepsilon}_s = X_i - \underline{X}_s \quad (4)$$

The values produced represent the magnitude of the T_(avg-mly-min) and T_(avg-mly-max) for every month of July from 1944 to 2009. A positive magnitude represents a year where the T_(avg-mly-min) or the T_(avg-mly-max) was above average. Conversely a negative magnitude represents a year where the T_(avg-mly-min) or the T_(avg-mly-max) was below average. A normal year will show similar magnitudes for both T_(avg-mly-min) and T_(avg-mly-max). When differing magnitudes are repeatedly observed, an UHI could be present. The next step was to determine if differing trends found using the deviation statistic were significantly different. These were examined using the Student's *t*-Test in the next analysis.

Student's *t*-Test

This research will use a two-tailed independent two-sample *t*-test. An independent two-sample *t*-test requires equal sample sizes. This study will use the results from the deviation statistic calculated from the previous procedure. μ_{tL} was used to represent the deviations for average monthly minimum temperature and μ_{tH} was used to represent the deviations for average monthly maximum temperature. The variances between the two groups are assumed equal ($\mu_{tL} = \mu_{tH}$). A Student's *t*-distribution was used to calculate the p-value. For this study a α-value of 0.05 will be used to test for significant difference. If the α-value is below the threshold of 0.05, then the null hypothesis (H_o) is rejected in favor of the alternative hypothesis (H_A) (see below).

$$H_o: \mu_{tL} = \mu_{tH}$$

$$H_A: \mu_{tL} = \mu_{tH}$$

This will test if the T_(avg-mly-min) and T_(avg-mly-max) are outside of the acceptable range for the local climate (Hawkins, Brazel, Stefanov, Bigler, & Saffell, 2003). Consecutive p-values below the 0.05 threshold will show long-term compromise to local climate records. Two equations must first be calculated to compute a *t*-test. To use a *t*-test, the data must first be standardized. The standard deviation is calculated using the following equation (Equation 5):

$$S_x = \sqrt{(1/N\,[(x_1 - \mu)^2 + (x_2 - \mu)^2 + \ldots + (x_N - \mu)^2])} \qquad (5)$$

, where $\underline{X}$ was inferred for μ (see Equation 1)

A standard deviation was used to determine the variability from the average.

The next step is to calculate the standard deviation of both groups (Equation 6). Where S_{x1}= standard deviation of T_(avg-mly-min) and S_{x2}= standard deviation T_(avg-mly-max).

$$S_{x1x2} = \sqrt{(1/2(S^2_{x1} + S^2_{x2}))} \qquad (6)$$

The final statistic used is the *t* statistic (Equation 7). This test will determine if the means are different. The variables are defined as follows: $\underline{X}_1$ = 20 point T_(avg-mly-min), $\underline{X}_2$ = 20 point T_(avg-mly-max), S_{x1x2} = grand standard deviation, n = sample size.

$$t = (\underline{X}_1 + \underline{X}_2)/(S_{x1x2}*\sqrt{(2/n)}) \qquad (7)$$

The final output of this test will produce a 20 point moving average of p-values. Significant difference observed using a 20 point moving average will show compromise to historical local climate data. The *t*-test will confirm differing trends found using the deviation statistic. The next statistic used for this research will attempt to identify if a linkage between land-use change and temperature trends exist. The final statistic used was the correlation statistic.

Correlation

The Pearson product-moment correlation coefficient (Pearson's correlation) was the final statistic test used in this research. This test will measure the correlation between two variables (T_(avg-mly-min) or T_(avg-mly-max) with commercial/industrial land-use). Mentioned previously, T_(avg-mly-min) and T_(avg-mly-max) were acquired from the NCDC. The commercial/industrial land-use data was acquired from public land records. This data was collected from four separate county GIS departments (Guilford, Mecklenburg, Wake, and Durham). Once the data was collected, a query was required to select only commercial/industrial parcels. These were chosen because they contribute the most to UHI formation (Lee & French, 2009). Land records were used because the records are public. By accessing these records, information regarding when a parcel was developed is permanently recorded. This was important because average monthly temperature were also measured yearly. The land records began in the early 1900's allowing for comparison with yearly climate records.

The commercial/industrial parcels were sorted using a selection by attributes query in a GIS. After the parcels were selected, two fields were chosen for the Pearson's correlation. The selected fields were 'build-year' (year parcel was improved) and land-area (in acres). A yearly record of developed commercial/industrial parcels will permit the ability to produce a running total of developed acreage with time. This will be used to determine if a linear relationship exists with local climatic trends.

This study uses the Pearson's correlation. This equation is defined as the covariance ($cov\ (X,Y)$) of two random variables divided by the product of their standard deviations ($\sigma_x\sigma_y$). The equation is as follows (Equation 8):

$$\rho_{X,Y} = (cov\ (X,Y))/(\sigma_x\sigma_y) = (\mathrm{E}[(\mathrm{X} - \mu_\mathrm{X})(\mathrm{Y} - \mu_\mathrm{Y})])/(\sigma_x\sigma_y) \qquad (8)$$

The Pearson's coefficient produces values between 1 or -1. A positive correlation is found for values ≥ 0.10 and a negative correlation for values ≤ -0.10. No correlation is found for values between -0.09 to 0.09. The T_(avg-mly-min) and commercial/industrial land-use will be correlated in an excel spreadsheet. Also, the T_(avg-mly-max) and commercial/industrial land-use will be correlated in an excel spreadsheet. The two outputs will be compared on a single scatter plot diagram using separate color symbols. Additionally, two trend lines will be added showing the sign and strength of correlation for the two separate outputs. (R^2) values will be added to the diagrams to display the correlation strength of each trend line. This statistic was used to test if a positive relation exists for T_(avg-mly-min) with commercial/industrial land-use, but not for T_(avg-mly-max) and commercial/industrial land-use. If a relationship is found with T_(avg-mly-min), but not with T_(avg-mly-max) then it can be assumed that the UHI effect is directly related to the land-use change adjacent to the airport. A raster data model will be used to find suitable sites for a new weather station in the second part of the methods.

Raster Data Model Using Pass/Fail Screening to Locate Suitable Sites For Alternate Weather Stations

This study incorporated two unrelated methodologies related to the investigation of an UHI at PTIA. The first goal was to identify the presence of an UHI and determine its impact on local climate. No prior research has been done on the UHI at PTIA; therefore the first methodology was required to establish the need for the second, main, methodology. The main goal will apply a GIS to find 'ideal' sites for weather stations.

‘Ideal’ sites are locations that are representative of the climate for their region (WMO, 2006). Studying past research, no work has been done related to site suitability of weather stations using a GIS. The majority of UHI research involves atmospheric modeling or mitigation practices (Baik, J. Kim, Y. Kim, & Han, 2007; Fast, Torcolini, & Redman, 2005; Niino, Mori, Satomura, & Akiba, 2006).

A GIS will be applied following criteria given by the World Meteorological Organization (WMO). The WMO identifies required siting criteria for weather stations that are representative of regional climate (WMO, 2006). In general, airports meet most if not all WMO criteria due to their large area and openness (WMO, 2006). This openness allows for air to mix at the surface and represent regional temperature. The present state of KGSO offers suitable information for aviation meteorology, but not for the region (WMO, 2006). KGSO is part of a synoptic scale network (100 km – 3000 km) (WMO, 2006). The purpose of a synoptic scale weather station is to measure meteorological data representative for the surrounding region. An UHI is considered a toposcale phenomenon which is considerably smaller compared to the synoptic scale (3 – 100 km) (WMO, 2006). The UHI effect will impact the weather station by recording data different than what would be expected for the region. The UHI is non-reversible because the land-use change is permanent; however, an alternative to overcome this problem will be conducted through a GIS analysis. The locations found acceptable in the GIS analysis will closely resemble the climate at KGSO prior to development.

Recognizing the causes of an UHI will serve as failing criteria in locating potential new sites for weather stations. Examples of failing criteria include roadways, development, steep slopes, forests, etc. Failing criteria cause microclimate conditions that are not representative of the region.

This portion of the methodology will define the raster data model and how raster data represents objects in space. A raster data model defined by ESRI is "A representation of the world as a surface divided into a regular grid of cells. Raster models are useful for storing data that varies continuously, as in an aerial photograph, a satellite image, a surface of chemical concentrations, or an elevation surface (ESRI, 2011)." Raster data uses cells to represent objects in space. For example, elevation data can be represented as values on a grid. Each cell will have a specific value to represent elevation at that location. An important concept of raster data is cell size. Cell size has a direct relation to the spatial resolution of the model (Kar & Hodgson, 2008). Smaller cell sizes equates to higher resolution, while a larger cell size will produce a coarser resolution (Kar & Hodgson, 2008). For this study cell size is not an issue for the spatial scale in use. This is due to synoptic weather stations being located in large, flat open-spaces (WMO, 2006). In raster data modeling, the cell size output is determined by the lowest spatial resolution dataset incorporated into the model. The coarsest grid for this model is 30 meters (~98.4 feet). This will be the cell size of the final model output. The spatial size of a weather station site is 10 meters by 7 meters (WMO, 2006). The 30 meter model output will fulfill this requirement.

Raster data models can be used to represent quantitative or qualitative data in space (Kar & Hodgson, 2008). The model used in this research will incorporate both. An example of quantitative data is elevation and an example of qualitative data would be land-use. For qualitative datasets, class definitions are provided to understand what a cell value represents (ex. NLCD 2006 71 = Grasslands/Herbaceous Land-use). Raster data models can only process raster data. Sometimes a dataset may only be available as a feature dataset (ex. points, lines, polygons). In the event of this, ArcGIS has a tool to convert datasets from feature to raster.

When locating a new weather station guidelines must be followed in order to represent the surrounding climate of a region (WMO, 2006). The first guideline comes from the NCDC's recommendations for locating Cooperative Stations. These guidelines state "A station in this network can be one site or a series of sites whose locations fall within 2 miles horizontal or 100 feet vertical difference (NCDC, 2011, Cooperative Stations)." The vertical requirement can be met using elevation data; however, the horizontal component cannot be met. Previously discussed, a map of KGSO (Figure 1) showed the commercial/industrial development covers a considerable amount of area inside the 2.5 mile buffer. To locate a new weather station inside 2 miles would not resolve the current climatic influence of the UHI effect at PTIA. The NCDC has additional criteria when the 2 mile horizontal component cannot not the fulfilled. They explain, "There are exceptions to this rule, with 'climatic compatibility', as determined by the NWS field manager, being the overriding factor (NCDC, 2011, Cooperative Stations)." For this study the raster data model will select potential new sites. This researcher will serve as the field manager for determining the 'climatic compatibility' of the selected sites.

This study used criteria from both the NCDC and the WMO. The criteria from the NCDC is already quantified, so little work is required to define these factors in the raster data model. The guidelines given from WMO Manuel (Appendix F) were not already quantified. Instead the WMO used descriptive criteria. These criteria have room for interpretation, which could lead to some bias by the researcher. Nonetheless, the criteria will be quantified as close as possible to the WMO Manuel. It is possible some locations could pass, but are unacceptable sites for an ASOS weather observation. Conversely, acceptable sites could fail to pass due to data interpretation or data quality. The model output should find most of the acceptable sites. This model will save time searching for acceptable new weather observations through the aid of spatial analysis.

The raster data model will be a site suitability model using pass/fail screening. This model uses a set of defined factors in a raster multiplication. For each factor, cells will be assigned either a 0 (failing factor) or a 1 (passing factor) (Kar & Hodgson, 2008). The equation for pass/fail screening is as follows:

$$EQUATION\text{: } Score = FC_1 * FC_2 * \ldots *FC_n \qquad (9)$$

FC represents the factor constraint for each criterion (Kar & Hodgson, 2008). All the factors multiplied for each cell will either result in a 1 or 0. All factors must pass in order for the score to equal 1. The following factors will be considered in the table below (Table 1). In total, eight factors will be analyzed in this model.

Table 1

Raster Data Model Factor Constraints

Factors	Comment	Reference
Elevation	(+/-) 100 feet	NCDC, 2011
Masked Region	≥ 2 miles AND ≤ 15 miles	NCDC, 2011
Slope	≤ 2%	WMO, 2006
Land-use	Acceptable Land-use 71,81,82	WMO, 2006
Impervious Buffer	500 feet around 21, 22, 23 or 24	WMO, 2006
Tree-line Buffer	393.7 feet around 41, 42 or 43	WMO, 2006
Water Buffer (raster)	492.1 feet around 11	WMO, 2006
Water Buffer (feature)	500 feet around Streams	WMO, 2006

Note: The eight factors listed are minimum site criteria defined by the National Climatic Data Center and the World Meteorological Organization. These criterion and quantified as close as possible to reflect real objects at the surface.

The first factor quantified is elevation defined by the NCDC. 901 feet is the elevation of the ASOS site for KGSO. This elevation was determined from a digital elevation model (DEM) from the North Carolina Department of Transportation. Values within +/-100 feet will pass this factor. Appendix F requires a station be located on level ground. For this factor location with a slope ≤ 2 % (also derived from the DEM) were considered acceptable.

Stations should be located in flat, open areas. The following qualitative data were gathered from the National Land Cover Database (NLCD) 2006 provided by the USGS. This dataset is a rasterized image representing different types of land-use. Land-use associated with openness are 71 (Grasslands/Herbaceous), 81 (Pasture/Hay), and 82 (Cultivated Crops).

A buffer of 500 feet was placed around land-use values 21, 22, 23, and 24 using the NLCD 2006 dataset. These classes were various densities of urban development. According to the WMO Manuel "the site should be well away from buildings, walls, or other obstructions (WMO, 2006)". Locations inside these buffer values fail. The site should also be well away from trees. A Euclidean distance (raster buffer tool) was used around land-use classes 41, 42, and 43 from the NLCD 2006 dataset. These values represent forested areas. The buffer used was 120 meters (393.7 feet).

Sites should be away from hallows due to cold air drainage and also away from bodies of water. A Euclidean distance of 150 meters (492.1 feet) was used around the land-use value 11 from the NLCD 2006 dataset. A 500 foot buffer was used around the feature layer representing streams provided by Guilford County GIS. This layer was then converted to raster data for analysis. It was assumed using the slope constraint, the Euclidean distance from water bodies, and the buffer from streams would remove areas impacted by cold air drainage (hallows).

The final factor is the spatial extent. Potential sites needed to be beyond 2 miles from KGSO, but the model should not look too far to avoid climate incompatibility. An arbitrary value of 15 miles is the furthest extent analyzed from KGSO. Locations within 2 miles or beyond 15 miles fail in this model.

The model output will be analyzed using aerial photography (provided by NC OneMap) for acceptability. The final output will likely have many passing locations. Most of these locations will be very small in spatial size. It is safe to assume larger passing locations (groups of passing cells) will be more representative of regional climate than smaller groups of passing cells. According to the WMO Manuel, "The optimum area is approximately 1 ha" (2.47 acres) for a weather station site (WMO, 2004, p. 9). In GIS the passing locations will be converted to features. From there the geometries of passing locations will be calculated. Using the select by attribute tool, locations ≥ 2.47 acres will be selected for individual analysis.

Points will be assigned to represent theoretical stations for each of these sites. Buffers of 300, 500, 750, and 1000 feet will be analyzed for each potential site. This will be compared with the 2010 North Carolina aerial photograph to determine site acceptability. If sites had objects (trees, buildings, ponds, etc.) within 300 feet, then these sites were excluded. Sites that appeared 'ideal' from the GIS analysis will be field tested to determine how well the model performed using the available data.

CHAPTER IV

RESULTS AND DISCUSSION

Statistical Output Confirming the Presence of an UHI

Deviation

Results were analyzed for the deviation statistics of KGSO, KCLT, and KRDU to test for decoupling. A 10 year moving average was used to find warming or cooling trends.

The trend in Figures 4 and 5 showed a decoupling of T_(avg-mly-min) from the T_(avg-mly-max) at KGSO. The decoupling occurs after 1995 for the month of July (Figure 4) and also for the 3 month temperature average (Figure 5). The T_(avg-mly-min) remained above normal, while the T_(avg-mly-max) showed a cooling trend. Recent years showed T_(avg-mly-min) were on average 1.5 Fahrenheit warmer compared to T_(avg-mly-max). This confirms the change seen with the latest Climate Normals for 1981 – 2010 (Appendix A). The UHI effect is not limited to just July, but encompasses the entire three-month period (June, July, and August). There was a period of warmer T_(avg-mly-max) during the 1950s and 1960s. However, this is present for all three stations. Instrumentation during that time could have been different or the climate for the region could have been drier.

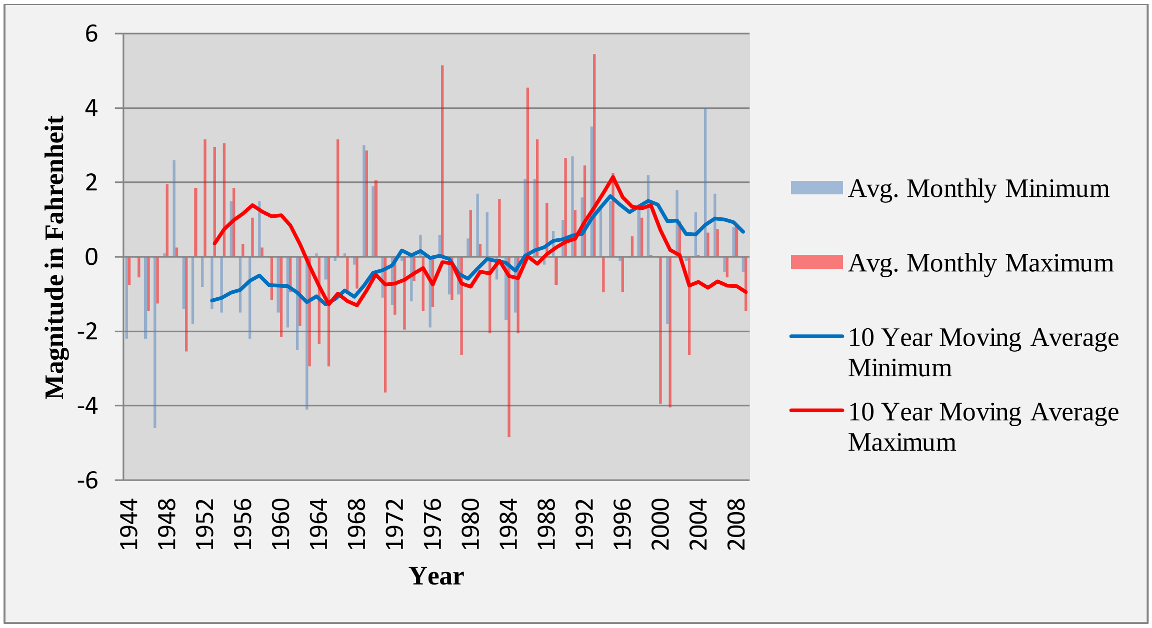

Figure 4. KGSO July Temperature Deviations. KGSO T_(avg-mly-min) and T_(avg-mly-max) for July were obtained from the NCDC and compared using statistical deviations to show long-term trends.

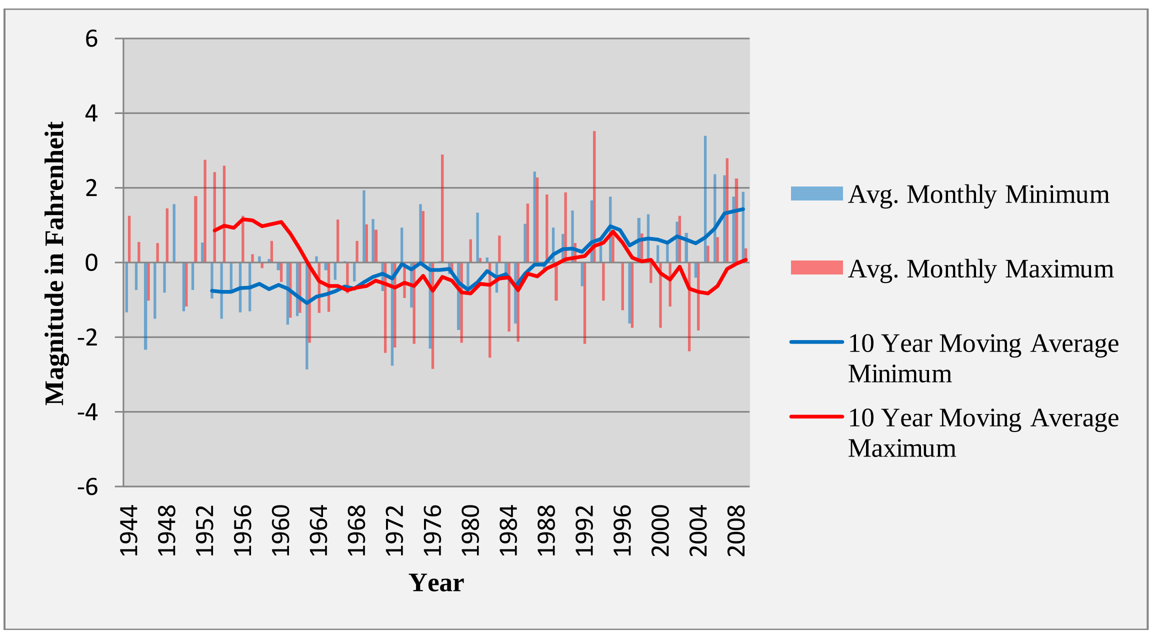

Figure 5. KGSO June, July, and August Temperature Deviations. KGSO T_(avg-mly-min) and T_(avg-mly-max) for June, July, and August were obtained from the NCDC and compared using statistical deviations to show long-term trends.

For KCLT no sign of decoupling was observed for July (Figure 6) or the 3 month average (Figure 7). This is representative of a normal ASOS observation (WMO, 2006). Both T_(avg-mly-min) and T_(avg-mly-max) entered a cooling trend around 1995. This trend differs from KGSO. KGSO showed only T_(avg-mly-max) in a cooling phase.

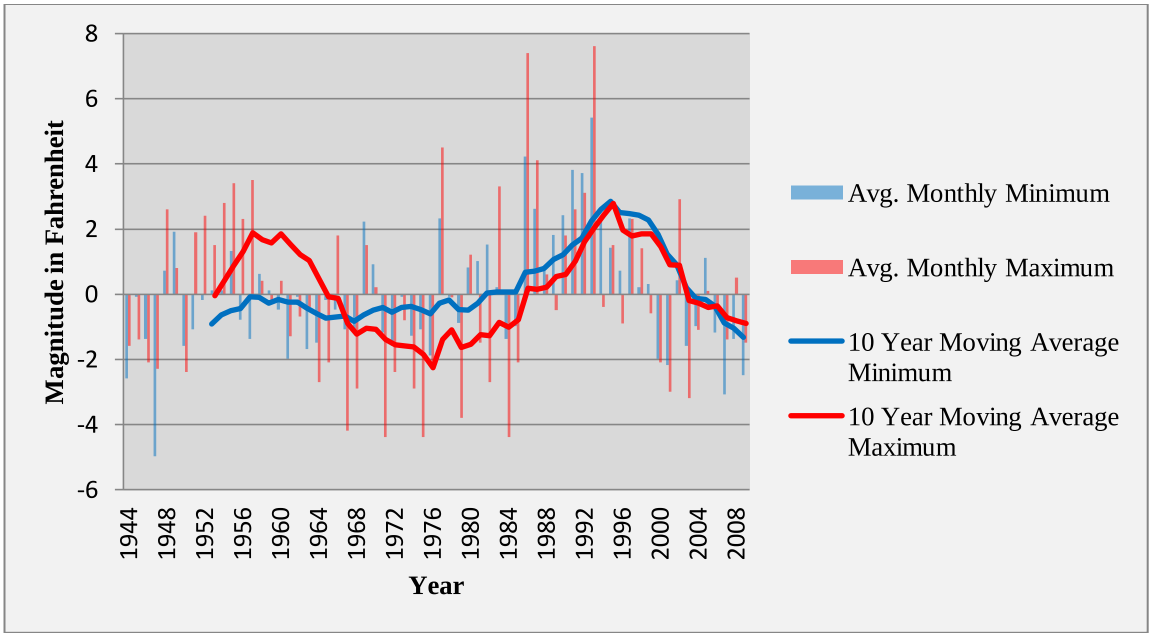

Figure 6. KCLT July Temperature Deviations. KCLT T_(avg-mly-min) and T_(avg-mly-max) for July were obtained from the NCDC and compared using statistical deviations to show long-term trends.

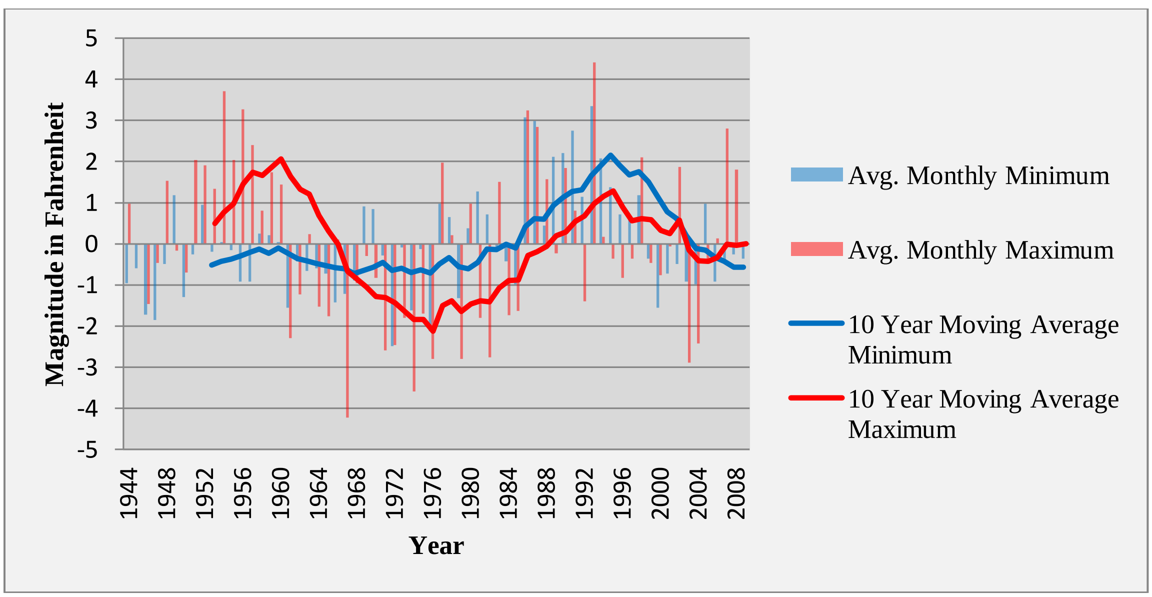

Figure 7. KCLT June, July, and August Temperature Deviations. KCLT T_(avg-mly-min) and T_(avg-mly-max) for June, July, and August were obtained from the NCDC and compared using statistical deviations to show long-term trends.

KRDU showed no decoupling for July (Figure 8) or for the 3 month average (Figure 9). This observation showed a slight cooling trend for T_(avg-mly-min) and T_(avg-mly-max) for July, but this was not as sharp as the cooling for KCLT. For the 3 month average, this site had an increase for both T_(avg-mly-min) and T_(avg-mly-max). It is possible that this observation is well located and is detecting global, not local, climate change. For the purposes of this analysis it does not appear to be under the influence of a classic urban heat island effect.

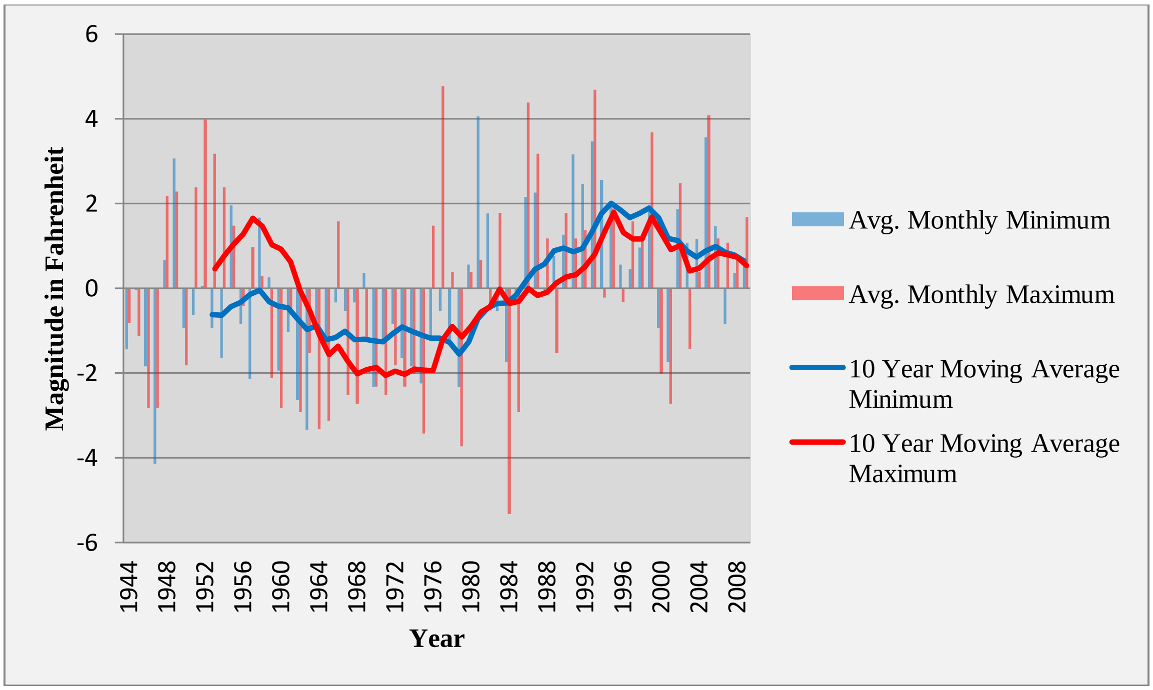

Figure 8. KRDU July Temperature Deviations. KRDU T_(avg-mly-min) and T_(avg-mly-max) for July were obtained from the NCDC and compared using statistical deviations to show long-term trends.

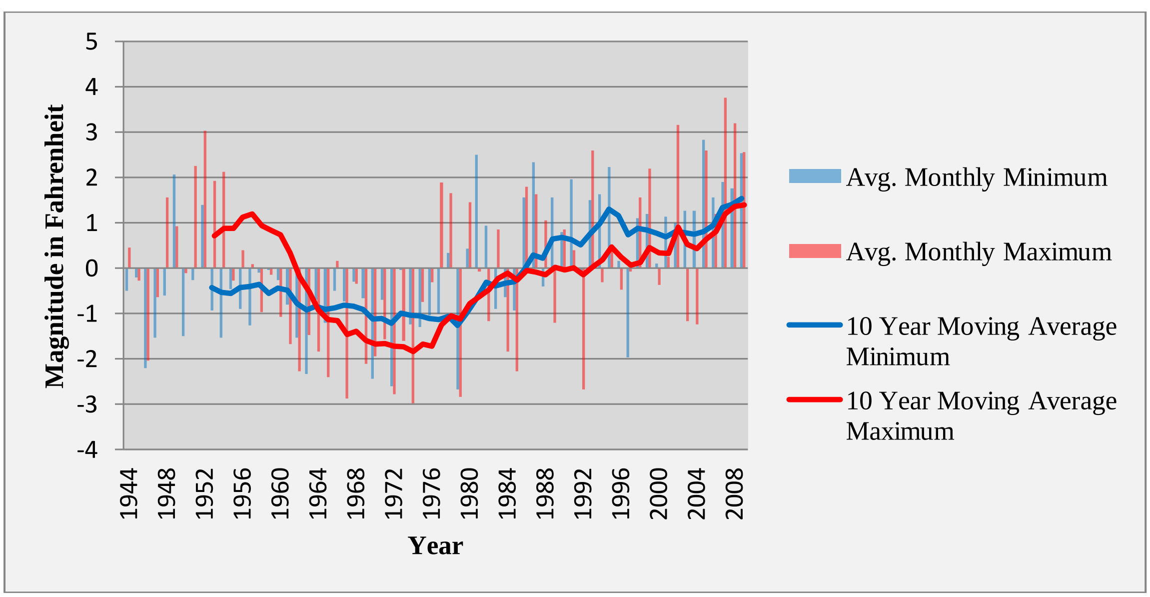

Figure 9. KRDU June, July, and August Temperature Deviations. KRDU T_(avg-mly-min) and T_(avg-mly-max) for June, July, and August were obtained from the NCDC and compared using statistical deviations to show long-term trends.

Student's *t*-Tests

The next set of results will analyze the *t*-test for significant difference between T_(avg-mly-min) and T_(avg-mly-max) for KGSO, KCLT, and KRDU. For KGSO the *t*-test shows a significant difference (p-value < 0.05) since 2005 for July (Figure 10). The three-month period shows significant difference every year since 2003 (Figure 11). These two results further confirm the decoupling of the T_(avg-mly-min) and T_(avg-mly-max) do not represent synoptic climate. Significant difference is seen in the 1950s and early 1960s, but this is seen for all three observations. Stated earlier, T_(avg-mly-max) were much higher for all three stations at that time. The significant difference occurs after the decoupling seen at KGSO. This makes sense due to arrays of 10 years being used in the *t*-tests.

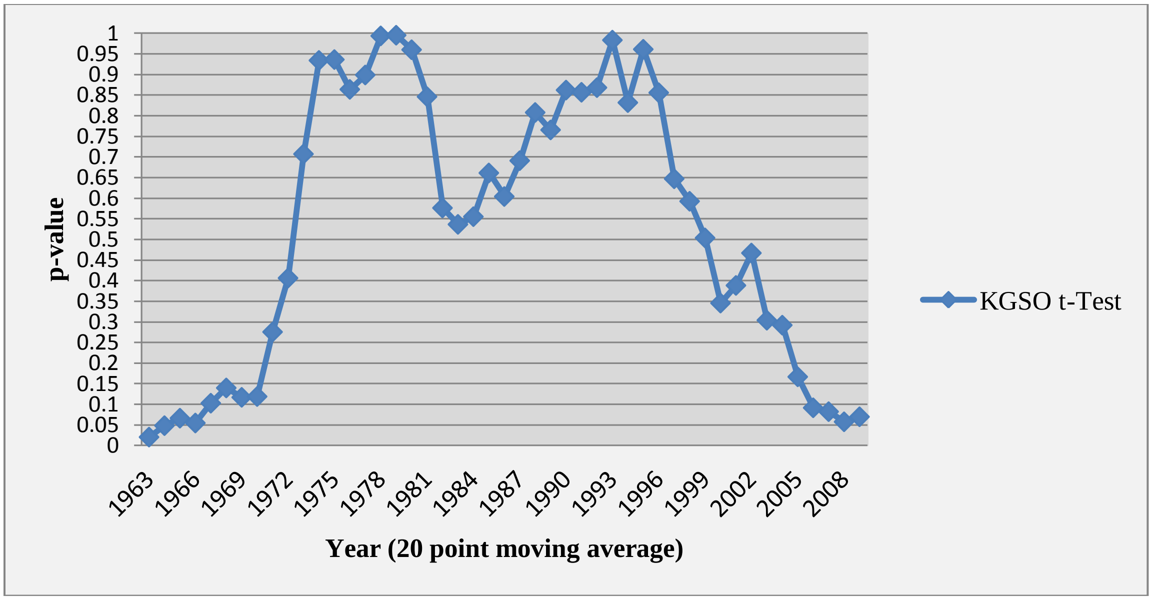

Figure 10. KGSO July Student's t-Test. KGSO T_(avg-mly-min) and T_(avg-mly-max) for July were compared using a two-tailed Student's t-*Test. Arrays of 20-years were used to find significant difference. Data obtained from the NCDC.*

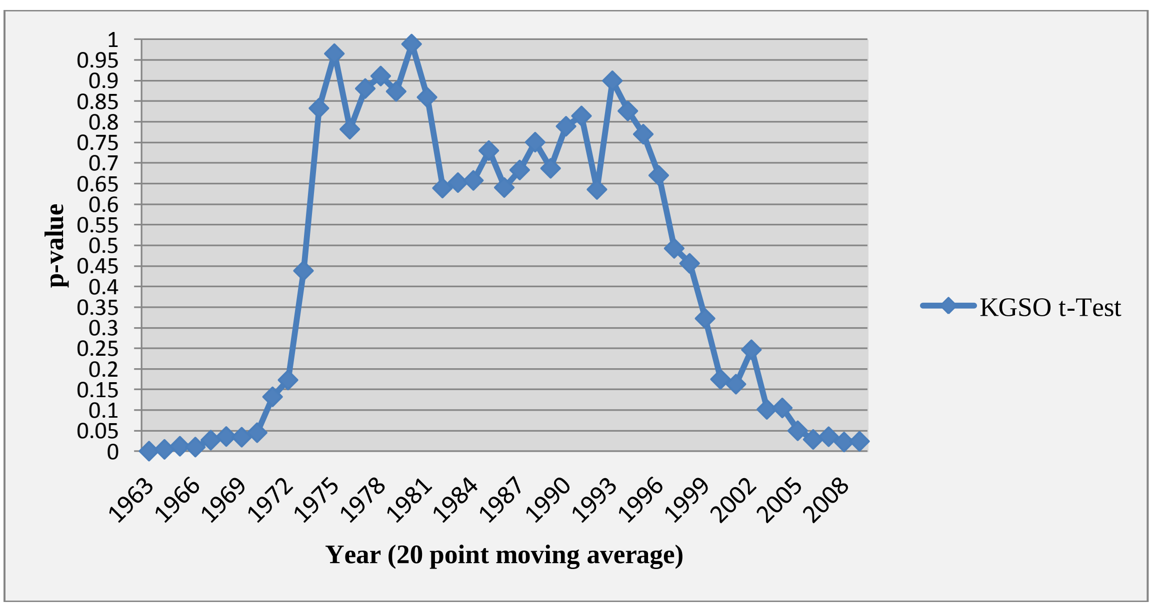

Figure 11. KGSO June, July, and August Student's t-Test. KGSO T_(avg-mly-min) and T_(avg-mly-max) for June, July, and August were compared using a two-tailed Student's t-*Test. Arrays of 20-years were used to find significant difference. Data obtained from the NCDC.*

For KCLT, the *t*-test is acceptable for the month of July (Figure 12). A startling feature is found in the data for the 3 month average *t*-test during the 1990s (Figure 13). The years from 1996 to 1999 showed p-values < 0.05 (significantly different). This data interruption returns to normal a few years later and appears to have no lasting effects. During 1997 and 1998 a strong El Nino Southern Oscillation (ENSO) was present for the region. Long lasting drought conditions were occurring during this period. This could have impacted summer climate for KCLT.

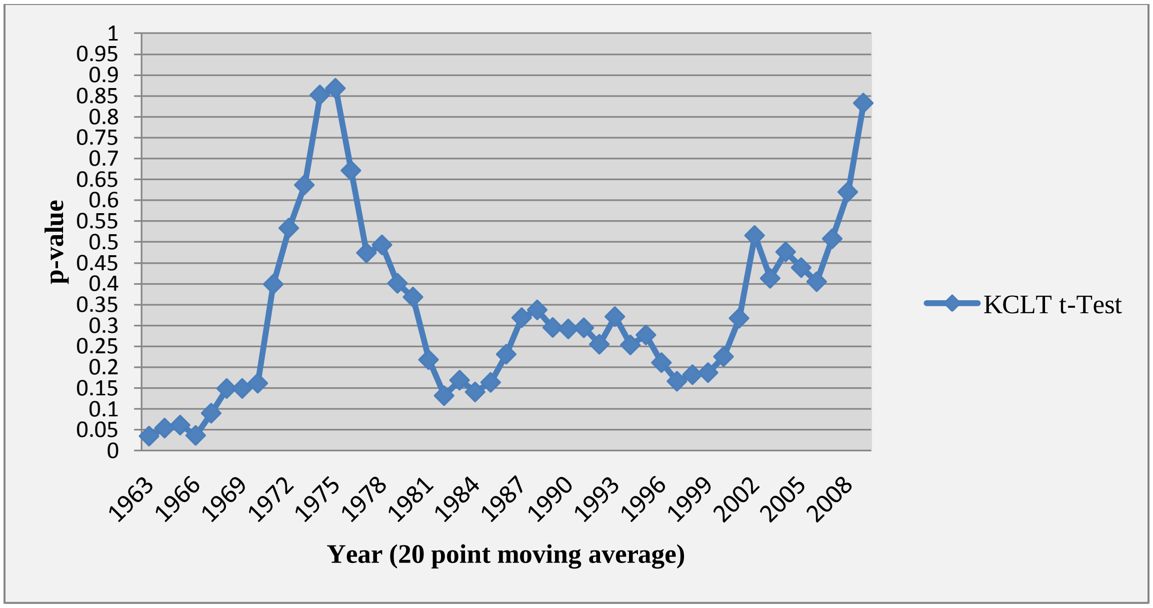

Figure 12. KCLT July Student's t-Test. KCLT T_(avg-mly-min) and T_(avg-mly-max) for July were compared using a two-tailed Student's t-Test*. Arrays of 20-years were used to find significant difference. Data obtained from the NCDC.*

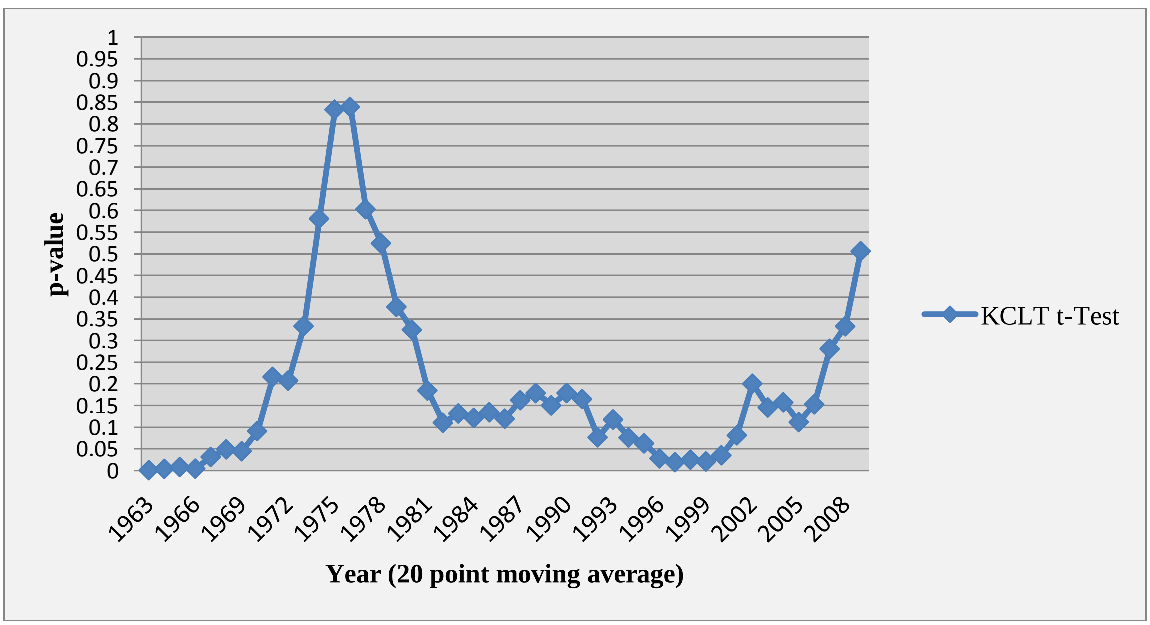

Figure 13. KCLT June, July, and August Student's t-Test. KCLT T_(avg-mly-min) and T_(avg-mly-max) for June, July, and August were compared using a two-tailed Student's t-Test*. Arrays of 20-years were used to find significant difference. Data obtained from the NCDC.*

The *t*-test showed acceptable p-values for KRDU for July (Figure 14) and the 3 month average (Figure 15). The KRDU ASOS is properly representing regional climate for its region.

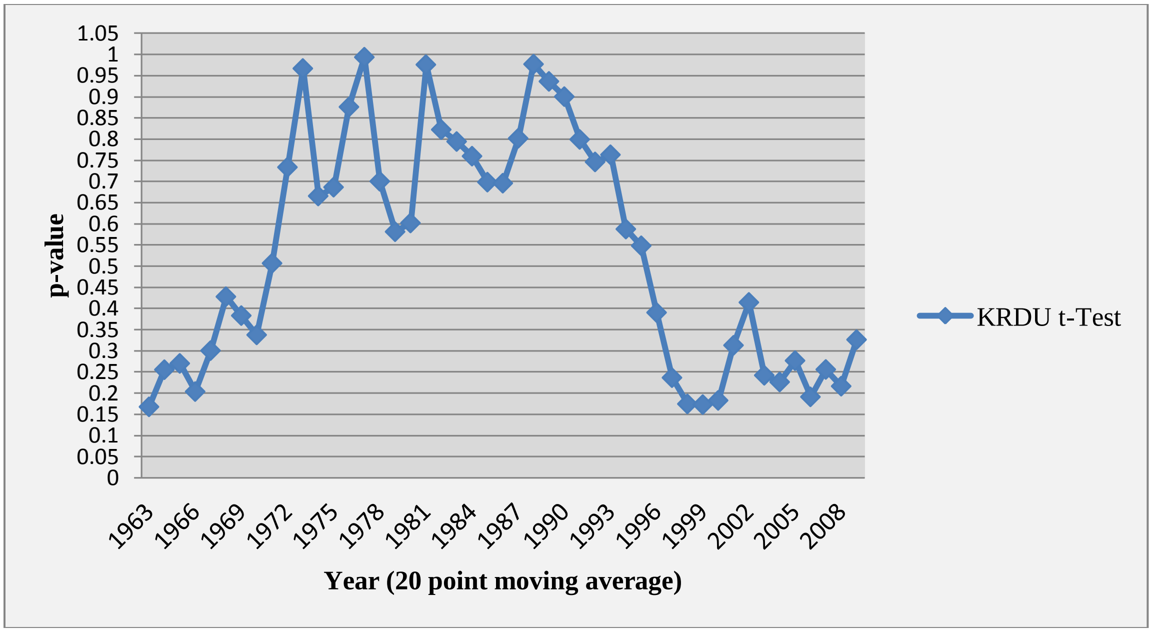

Figure 14. KRDU July Student's t-Test. KRDU T_(avg-mly-min) and T_(avg-mly-max) for July were compared using a two-tailed Student's t*-Test. Arrays of 20-years were used to find significant difference. Data obtained from the NCDC.*

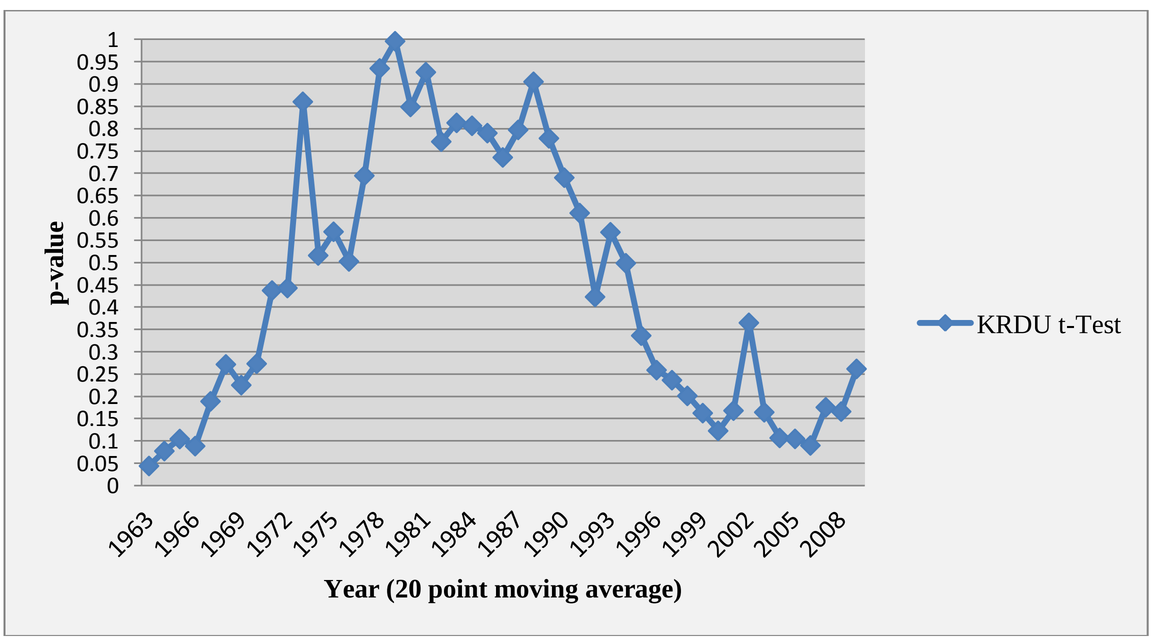

Figure 15. KRDU June, July, and August Student's t-Test. KCLT T_(avg-mly-min) and T_(avg-mly-max) for June, July, and August were compared using a two-tailed Student's t*-Test. Arrays of 20-years were used to find significant difference. Data obtained from the NCDC.*

Correlation

The final statistical analysis will determine whether a correlation exists between average minimum temperature and industrial/commercial parcels. A linear trend line is used to determine whether or not a correlation exists. The following graphs contain two independent variables. The vertical axis displays temperature in Fahrenheit and the horizontal axis displays total commercial/industrial land-use in acres. T_(avg-mly-min) and T_(avg-mly-max) will be displayed on the same scatter plot. Minimum temperatures will be represented by the color blue and maximum temperatures will be represented by red. A R^2 value will be included for each trend line. R^2 values ≥ 0.10 show a correlation while values ≤ 0.09 show no correlation.

For KGSO (Figure 16) a positive correlation is found for July T_(avg-mly-min) and industrial/commercial parcels with a R^2 value of (0.19). The T_(avg-mly-max) showed no correlation with a R^2 value of (0.0001). Figure 17 showed a stronger correlation for the 3 month T_(avg-mly-min) and industrial/commercial parcels with a R^2 value of (0.34). Again, the 3 month T_(avg-mly-max) (Figure 17) showed no correlation with a R^2 value of (0.00009). The correlation statistic for KGSO is in agreement with classic UHI research. T_(avg-mly-min) were influenced by impervious surface, whereas T_(avg-mly-max) showed no relationship.

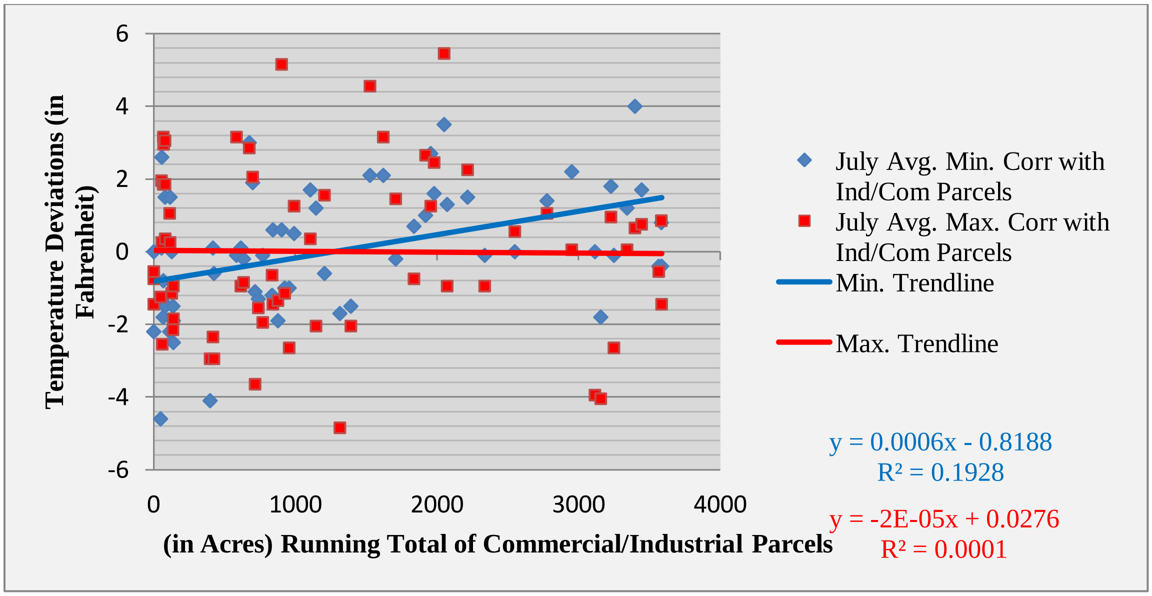

Figure 16. Correlation of July Average Monthly Min/Max Temperature with Ind/Com Parcels for KGSO. KGSO July T_(avg-mly-min) and T_(avg-mly-max) data obtained from the NCDC. Parcels representing impervious surface was obtained from Guilford County GIS. The two independent datasets were compared using a correlation statistic to find if a relationship exists.

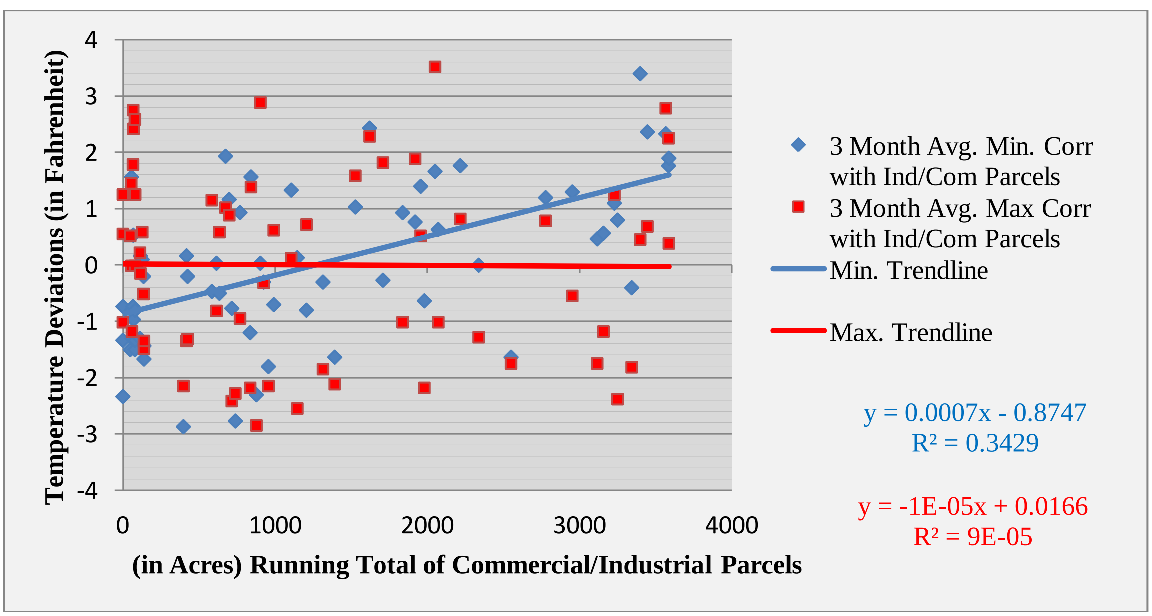

Figure 17. Correlation of June, July, and August Average Monthly Min/Max Temperature with Ind/Com Parcels for KGSO. KGSO June, July, and August T_(avg-mly-min) and T_(avg-mly-max) data obtained from the NCDC. Parcels representing impervious surface was obtained from Guilford County GIS. The two independent datasets were compared using a correlation statistic to find if a relationship exists.

For KCLT the T_(avg-mly-min) for July (Figure 18) showed no correlation with the industrial/commercial parcels with a R^2 value of (0.01). The T_(avg-mly-max) showed no correlation as well with a R^2 value of (0.0002). Figure 19 showed no correlation for the 3 month T_(avg-mly-min) and industrial/commercial parcels with a R^2 value of (0.0556). The 3 month T_(avg-mly-max) (Figure 19) showed no correlation with a R^2 value of (0.00001). The lack of correlation for the T_(avg-mly-min) or T_(avg-mly-max) with the industrial/commercial parcels indicate KCLT has no urban influence and represents climate for its region.

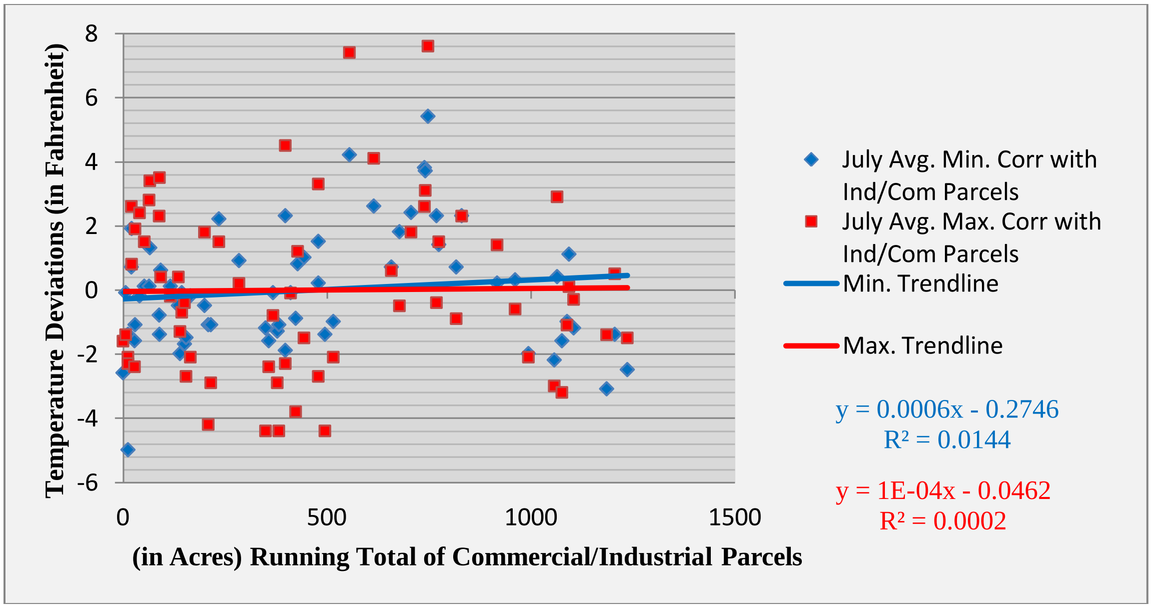

Figure 18. Correlation of July Average Monthly Min/Max Temperature with Ind/Com Parcels for KCLT. KCLT July T_(avg-mly-min) and T_(avg-mly-max) data obtained from the NCDC. Parcels representing impervious surface was obtained from Mecklenburg County GIS. The two independent datasets were compared using a correlation statistic to find if a relationship exists.

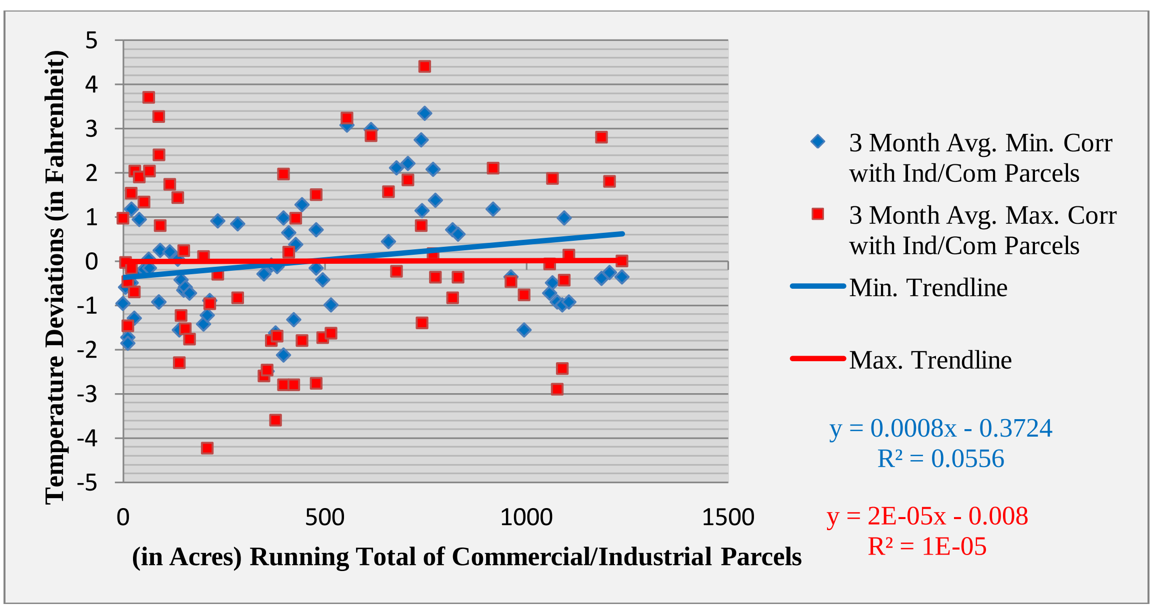

Figure 19. Correlation of June, July, and August Average Monthly Min/Max Temperature with Ind/Com Parcels for KCLT. KCLT June, July, and August T_(avg-mly-min) and T_(avg-mly-max) data obtained from the NCDC. Parcels representing impervious surface was obtained from Mecklenburg County GIS. The two independent datasets were compared using a correlation statistic to find if a relationship exists.

For KRDU the T_(avg-mly-min) (Figure 20) showed a positive correlation with the industrial/commercial parcels with a R^2 value of (0.17). The T_(avg-mly-max) (Figure 20) showed no correlation with a R^2 value of (0.0758). Figure 21 showed a stronger correlation for the 3 month T_(avg-mly-min) and industrial/commercial parcels with a R^2 value of (0.40). This time a positive correlation was observed between the 3 month T_(avg-mly-max) (Figure 21) with the commercial/industrial parcels with a R^2 value of (0.18). Normally the maximum temperature does not respond to land-use change. The results of the deviation and *t*-test showed no indication of an UHI effect at this site. It is likely KRDU is representing a larger-scale climatic change. Another explanation to the positive correlation at KRDU could be the time when development first began. 87.9% of the development around KRDU occurred after 1980. This fast-paced development along with above normal T_(avg-mly-min) and T_(avg-mly-max) could explain this correlation. However, this research is only interested in finding the link between minimum temperature and land-use change.

The results of the statistical analyses indicated an UHI effect is occurring at KGSO. The deviation statistic showed a decoupling of T_(avg-mly-min) from T_(avg-mly-max). This is a common result of weather stations impacted by an UHI. The Student's *t*-Test confirmed the decoupling seen in the deviation statistic was significantly different. The correlation statistic showed a positive connection between the commercial/industrial development with T_(avg-mly-min) but not with T_(avg-mly-max) for KGSO. This verifies prior research that minimum temperature responds to land-use change, but not maximum temperatures. Neither KCLT nor KRDU showed any indications of an UHI impacting their weather stations.

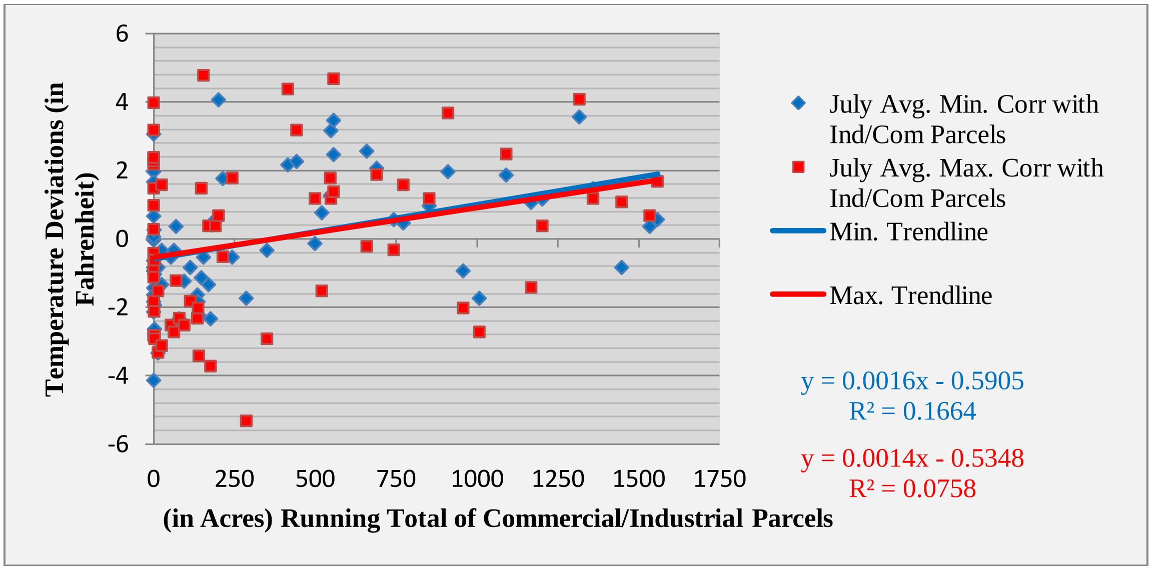

Figure 20. Correlation of July Average Monthly Min/Max Temperature with Ind/Com Parcels for KRDU. KRDU July T_(avg-mly-min) and T_(avg-mly-max) data obtained from the NCDC. Parcels representing impervious surface was obtained from Durham and Wake Counties GIS. The two independent datasets were compared using a correlation statistic to find if a relationship exists.

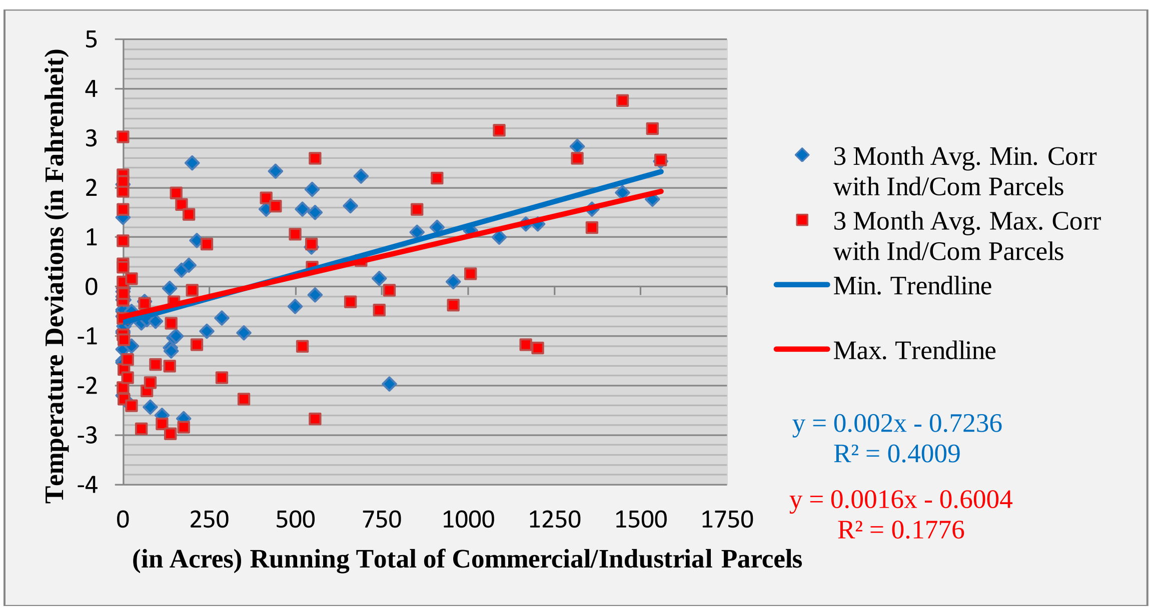

Figure 21. Correlation of June, July, and August Average Monthly Min/Max Temperature with Ind/Com Parcels for KRDU. KRDU June, July, and August T_(avg-mly-min) and T_(avg-mly-max) data obtained from the NCDC. Parcels representing impervious surface was obtained from Durham and Wake Counties GIS. The two independent datasets were compared using a correlation statistic to find if a relationship exists.

Locating Suitable Sites Using Raster Data Analysis

The final set of results in this research will determine suitable sites for a new weather station for KGSO. Before this analysis could proceed, some minor procedures were performed with the raster data model output. There were numerous individual raster cells that passed in the model output. These small cells were excluded from the analysis. The focus was placed on large contiguous (multiple passing cells grouped together) locations that passed the raster data model.

Finding the large contiguous passing sites requires converting from raster data to a feature dataset. This was done by using the raster to polygon tool in ArcGIS. Polygons ≥ 1 hectare was analyzed for verification (WMO, 2006). This was assuming large contiguous passing locations were likely to be better sites. 10 sites were found to be greater than 1 hectare. Additional procedures were performed to test suitability of these sites. These 10 sites were narrowed down by placing buffers around a central point of the polygon to test for openness. A multiple ring buffer analysis of 300, 500, 750 and 1000 feet were used in ArcGIS. Sites with obstructions within 300 feet were deemed non-suitable. Minor obstructions at the 500 foot range or beyond were noted to see if any problem arose with that particular feature. These included trees, ponds, buildings, etc. Obstructions are more likely to occur at greater ranges from the site; however, these obstructions would have less impact. The buffer analysis was used in comparison with the 2010 North Carolina State aerial photograph. This photograph is sub-foot (6 inch pixel resolution) and is very useful for locating and identifying any problems that may arise with a site.

The sites were further narrowed down using the aerial photograph to note features that would prove or disprove the model. New fields were added to the attribute table of the 10 sites selected (300, 500, 750 and 1000). The fields added represented the buffers in feet around each potential site. If no significant obstructions were observed, then a value of 1was entered into the new field. If an obstruction was observed (trees, buildings, water, etc.) then a value of 0 was entered. Sites with value of 1 at 300, 500, 750 and 1000 would be considered ideal. However, it is unlikely to have this scenario. Instead sites with a value of 1 for 300 and 500 would be acceptable and 750 would be superb. This narrowed the search down to seven sites. One of these sites was the White Street Landfill. This would not be a good site if the landfill reopens as expected. However, if this parcel were not to reopen and was preserved open-space, then this site could possibly serve as an alternative.

Instead the six other potential sites were investigated as field work. Two sites were southwest of KGSO, two to the south of KGSO, and two sites northeast of KGSO. The primary goal for the field investigation was to confirm the openness of the site and to observe how flat the site was. Any significant slopes observed could create microclimates if a station were located at the site, the primary one being cold air drainage. Slope can also impact wind measurement and the overall mixing of the air at the surface. Other surface objects were investigated, such as new construction, objects at the surface not seen on the aerial photograph, and anything else that could impact a weather station.

Photographs were taken at the six sites visited. These were captured as panoramas to visualize the extent of openness at the surface. This allows the viewer to see any obstructions, how flat the land is, and also how accessible is the land. The pictures were taken from roadways and directed towards where to the site would be. Five of these sites were private property. This is the reason for photographs being taken on easements off roadways. The research is to find suitable sites for alternate weather stations, not to implement them. However, this model could be used by the North Carolina State Climate Office or the National Climatic Data Center (NCDC) to address problems at weather stations with known artificial microclimates.

Suitable Sites

The first site (Figure 22) was located off High Point Road (Old U.S. 311) in the Kernersville Township. From the roadway this site had a noticeable upslope from the roadway (Figure 23). The site was open, but the slope on the southern end could have long-term impacts on surface winds. This would impact the mixing of temperature and dew point temperature at the surface. Because of this surface feature, this site would not be desirable for a weather station.

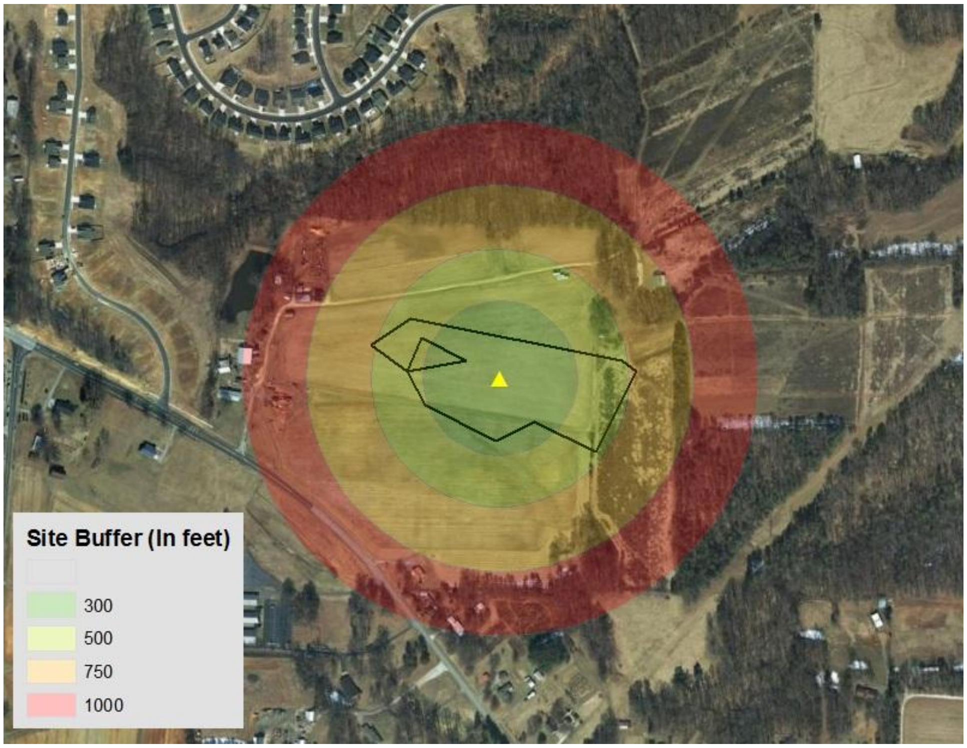

Figure 22. Suitable Site 1. 2010 North Carolina Orthoimagery for Suitable Site 1 (NC OneMap). The four ring buffers were produced in ArcGIS to determine proximity and density of obstacles to the suitable site. The yellow triangle represents the center of the suitable site and the buffer analysis. The black polygon represents the extent of the suitable site.

Figure 23. Suitable Site 1 Panorama. A panoramic view of Suitable Site 1 from the nearest roadway directed towards the center of the suitable site.

The second site (Figure 24) was located off Watkins Ford Road in the Kernersville Township. This site looked acceptable from the roadway (Figure 25) compared to Site 1. The landscape was very flat in all directions. The site was also very open. Surface vegetation appeared excellent for a weather station. The current use of this site is agricultural. Surrounding the site was low density residential with no commercial use nearby. The distance from KGSO is 7.77 miles. If the land-owner were willing to allow access to their farm, then this site could serve as an alternative to KGSO.

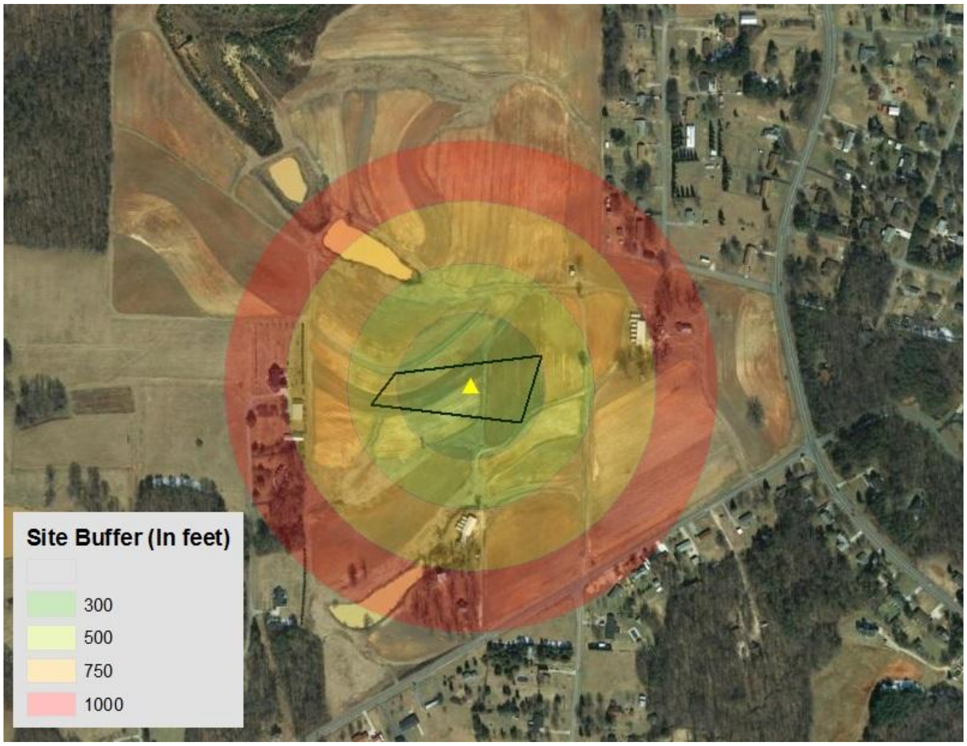

Figure 24. Suitable Site 2. 2010 North Carolina Orthoimagery for Suitable Site 2 (NC OneMap). The four ring buffers were produced in ArcGIS to determine proximity and density of obstacles to the suitable site. The yellow triangle represents the center of the suitable site and the buffer analysis. The black polygon represents the extent of the suitable site.

Figure 25. Suitable Site 2 Panorama. A panoramic view of Suitable Site 2 from the nearest roadway directed towards the center of the suitable site.

The third site (Figure 26) was located off Harlow Road in the High Point Extended Territorial Jurisdiction (ETJ). This site had some gentle rolling hills (Figure 27), but the slope was more lax compared to Site 1. Site 3 looked okay overall, but was not as open or flat as site 2. The site was 14.39 miles from KGSO, almost twice the distance of Site 2. This site was better than Site 1, but was not as good as site 2. If no other sites look acceptable, this could be an alternative.

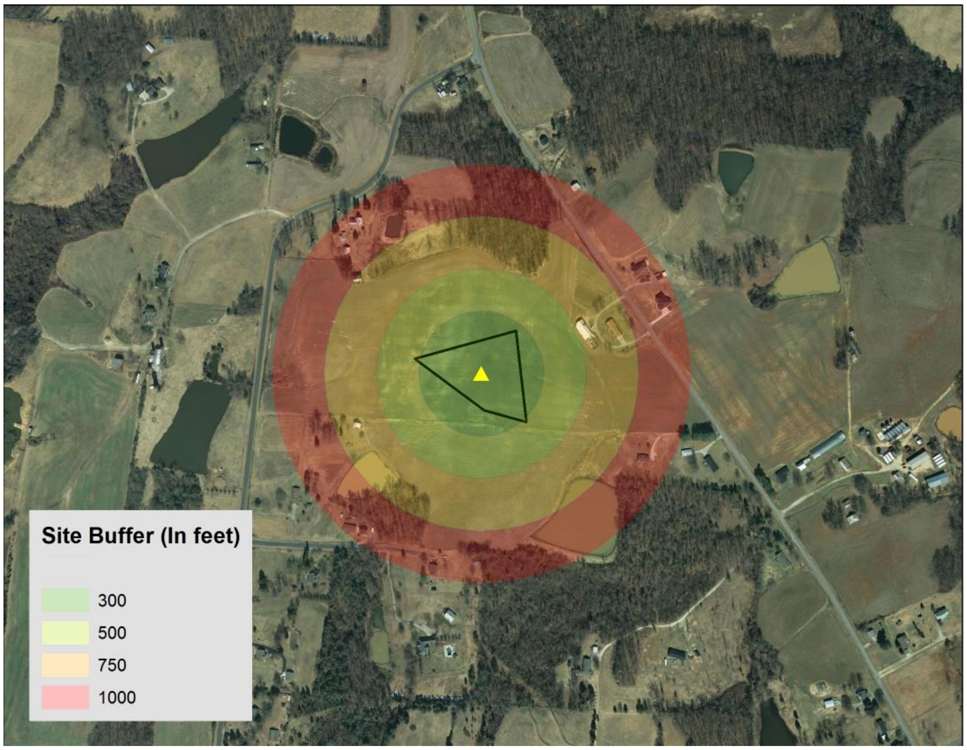

Figure 26. Suitable Site 3. 2010 North Carolina Orthoimagery for Suitable Site 3 (NC OneMap). The four ring buffers were produced in ArcGIS to determine proximity and density of obstacles to the suitable site. The yellow triangle represents the center of the suitable site and the buffer analysis. The black polygon represents the extent of the suitable site.

Figure 27. Suitable Site 3 Panorama. A panoramic view of Suitable Site 3 from the nearest roadway directed towards the center of the suitable site.

The fourth site (Figure 28) was located off Davis Mill Road in Pleasant Garden. Of all the sites, this was the largest contiguous open-space (Figure 29). Agricultural was the primary land-use for this site. No other land-use was within 2,000 feet, much greater in some directions, from this site. The open area was approximately 400 acres and is the reason why more than one area passed the raster data model in Figure 34. The site in the center of the image is site 4. Above site 4 was a potential site that had too many obstructions to the west and southwest. However, this additional passing site within reasonable distance of site 4 makes it a stronger candidate for a weather station. The openness of this would allow for good surface mixing on a regional scale. The site had some sloping on the periphery, but the potential site was on a level plateau in relation to the property as a whole. There were some minor rolling hills and a few obstructions (trees or a barn/other agricultural structure). In all, this site was very open and would have little surface bias in climate readings. The primary hindrance in this site is distance from KGSO (13.42 miles).

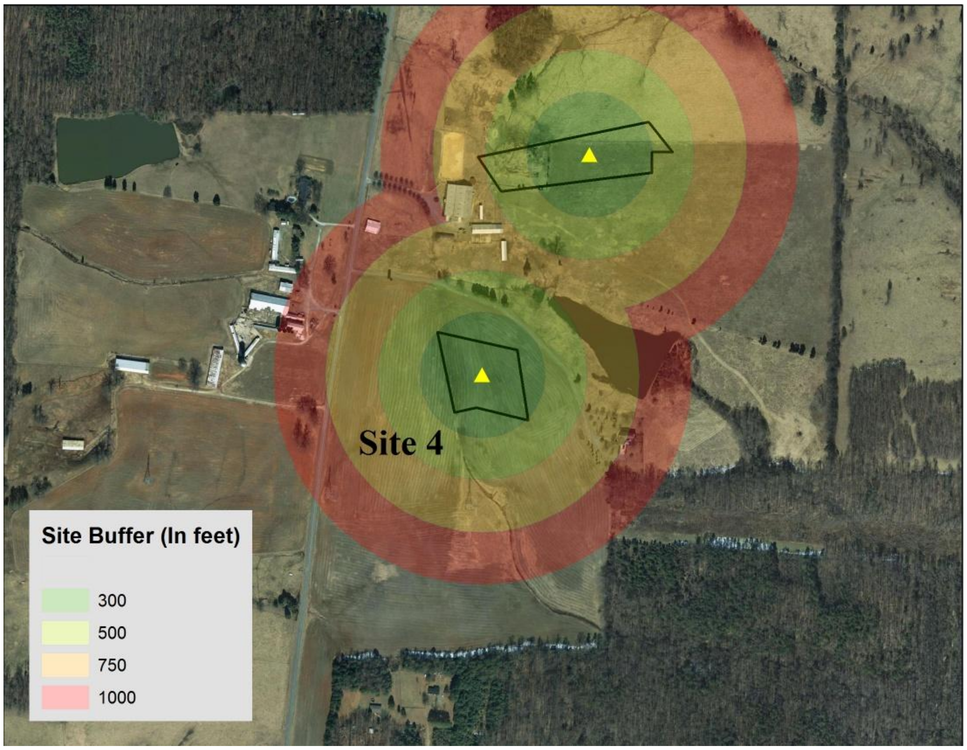

Figure 28. Suitable Site 4. 2010 North Carolina Orthoimagery for Suitable Site 4 (NC OneMap). The four ring buffers were produced in ArcGIS to determine proximity and density of obstacles to the suitable site. The yellow triangle represents the center of the suitable site and the buffer analysis. The black polygon represents the extent of the suitable site.

Figure 29. Suitable Site 4 Panorama. A panoramic view of Suitable Site 4 from the nearest roadway directed towards the center of the suitable site.

The fifth site (Figure 30) was located off North Carolina Highway 150 in Brown Summit. This site was very open and flat (Figure 31) similar to Site 2. The vegetation type and land-use looked ideal for a weather station. There were very few obstruction (just a few understory plants). The use was agricultural and the residential density was very low. No commercial land-use was nearby. This site is very similar to Site 2, except for distance. The primary limitation of this site would be distance from KGSO (14.25 miles).

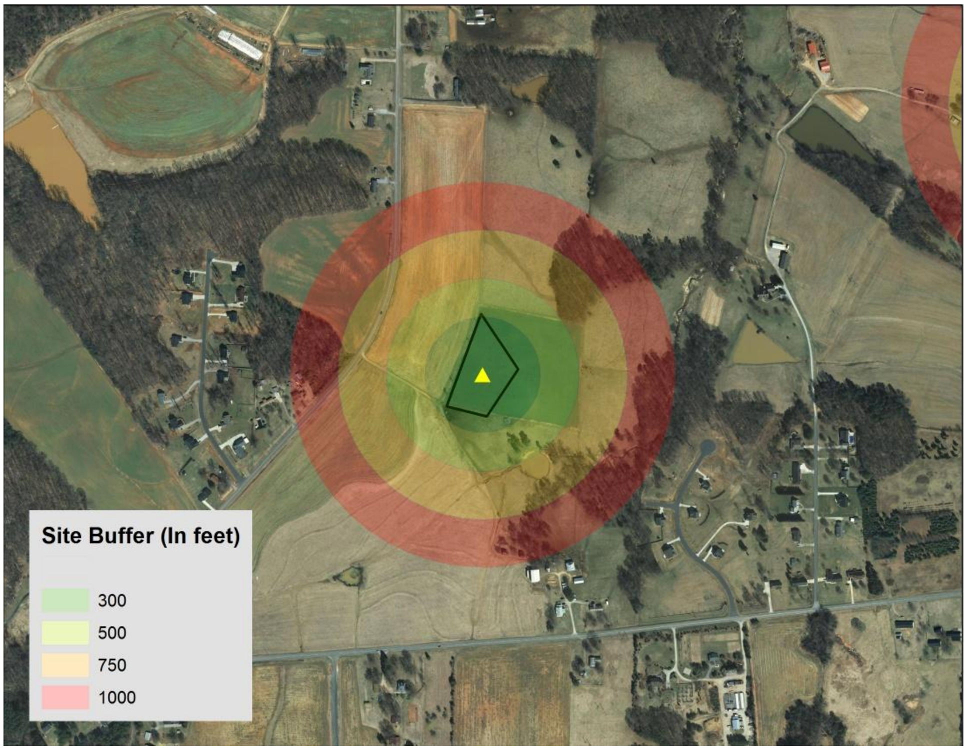

Figure 30. Suitable Site 5. 2010 North Carolina Orthoimagery for Suitable Site 5 (NC OneMap). The four ring buffers were produced in ArcGIS to determine proximity and density of obstacles to the suitable site. The yellow triangle represents the center of the suitable site and the buffer analysis. The black polygon represents the extent of the suitable site.

Figure 31. Suitable Site 5 Panorama. A panoramic view of Suitable Site 5 from the nearest roadway directed towards the center of the suitable site.

The sixth site (Figure 32) was also located off North Carolina Highway 150 in Brown Summit. This land parcel was the only government owned parcel of the six sites investigated. This parcel was acquired by Guilford County in 1998 through the Joseph Bryan Foundation. The first thing noticed was a wind sock at this site and a few small buildings (Figure 34). It turns out this site is used by the Greensboro Radio Aeromodelers Inc. (Figure 35). No record was found while doing research that this location was being used by this type of aircraft prior to visiting the site. This site was open and very flat and the vegetation type was suitable for a weather station (Figure 33). The land is preserved open space institutional amongst low-density residential land-use. There is some commercial use to the southeast of this site (~900 ft) and a church to the northeast (~700 ft). No other development is nearby. The main concern with this site is distance from KGSO (14.95 miles). Positives for this site include: government owned and already has aircraft use.

A personal communication was made with the president of the GRAMS, Grady Bare. He said, "A weather station would be beneficial to rc aeromodeling mostly for wind speed and direction. Any equipment would have to be placed behind our flight line" (G. Bare, personal communication, August 4, 2011). The public land-use zoning and rc aeromodeling make this site a solid candidate for an alternative weather station.

The raster data model in conjunction with the 2010 State Orthoimagery did well in locating potential sites using the factor constraints in the model and focusing on sites ≥ 1 hectare. Of the six sites visited, four of them were good candidates for a weather station. It is necessary to have more than one alternative. This will allow for options when communicating with private land owners regarding access to their property. Land owners have the right to allow or not allow access. Thus having more than one option is important. Additionally, having multiple passing ‘ideal’ sites could result in having more than one weather station added to the synoptic weather network. Multiple new weather stations will give better coverage of weather observations for the region.

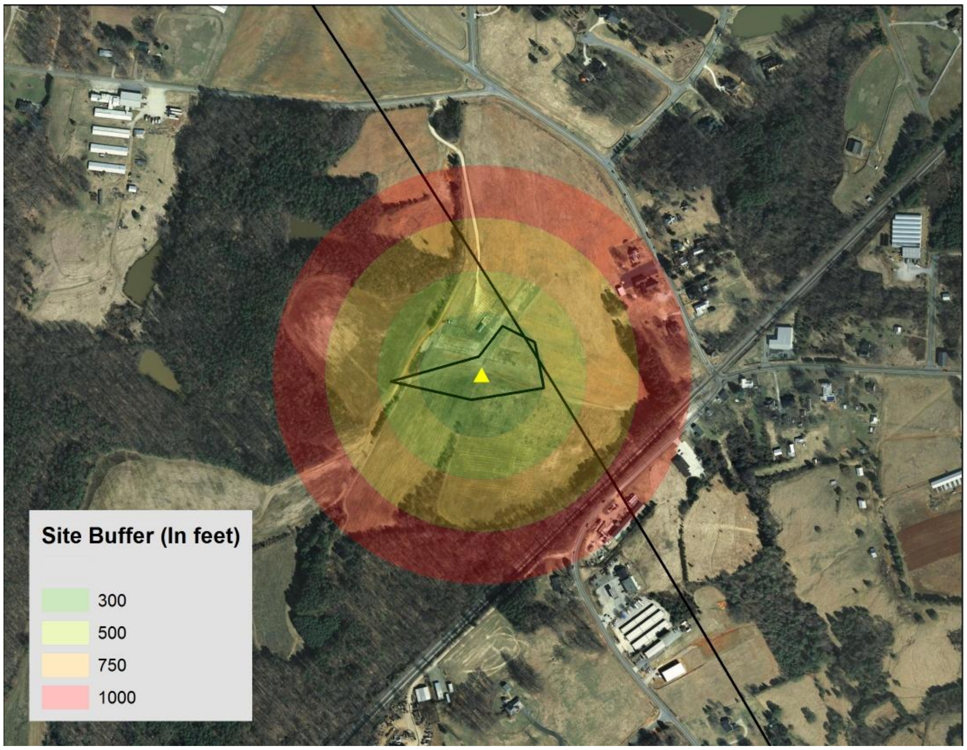

Figure 32. Suitable Site 6. 2010 North Carolina Orthoimagery for Suitable Site 6 (NC OneMap). The four ring buffers were produced in ArcGIS to determine proximity and density of obstacles to the suitable site. The yellow triangle represents the center of the suitable site and the buffer analysis. The black polygon represents the extent of the suitable site.

Figure 33. Suitable Site 6 Panorama. A panoramic view of Suitable Site 6 from the nearest roadway directed towards the center of the suitable site.

Figure 34. Greensboro Aeromodelers Airport. Buildings and wind sock used by the Greensboro Aeromodelers Inc.

Figure 35. Greensboro Aeromodelers Signage. Greensboro Aeromodelers Inc. signage at entrance.

CHAPTER V

SUMMARY, CONCLUSIONS, & SUGGESTIONS FOR FUTURE WORK

The primary goal of this research was to test if 'ideal' sites for weather stations could be located using available data in a GIS. This was applied to PTIA, due to a newly verified UHI effect at this ASOS site (see section "Statistical Output Confirming the Presence of an UHI"). The UHI effect was verified in this research by using three statistical procedures to examine T_(avg-mly-min) and T_(avg-mly-max) for three ASOS sites in North Carolina: KGSO, KCLT, and KRDU. These statistical procedures examined the months of July and a three-month period which included: June, July, and August for trends characteristic of an UHI effect. The first statistical test used a deviation statistic to detect decoupling of maximum and minimum temperature. The second statistic used a Student's *t*-Test to determine if the decoupling was significantly different from the long-term average. The third statistic used was a correlation statistic between T_(avg-mly-min) or T_(avg-mly-max) and total impervious surface. The final procedure in this research produced a raster data model to locate alternate weather station sites for KGSO.

All three weather stations showed a decoupling at the beginning of the 67-year time series (1944 – 2009) for T_(avg-mly-min) and T_(avg-mly-max). This trend goes away for all three stations during the 1960s. Towards the last 15-years of the time series, KGSO showed a decoupling of T_(avg-mly-min) from T_(avg-mly-max). The T_(avg-mly-min) trend was above average, while the T_(avg-mly-max) was below average. During the same period KCLT showed both T_(avg-mly-min) and T_(avg-mly-max) below average, while KRDU showed T_(avg-mly-min) and T_(avg-mly-max) above average. The trend seen at KGSO is representative of an urban heat island effect, while trends for KCLT and KRDU appeared to be normal for their respective regions.

A significant difference is observed at the beginning of the 67-year time series for all three weather stations. This was due to above average T_(avg-mly-max) observed at all three weather stations. No significant difference is observed again until the 1990s at the KCLT ASOS site. This is observed for the years 1996 – 1999. The significant difference disappears in the year 2000 and does not return. This was a surprising find for KCLT, but does not appear to have a lasting influence on local climate records for the KCLT region. A significant difference occurs for KGSO for the July T_(avg-mly-min). This difference began in 2005 and continues until 2008. The significant difference for the three-month period at KGSO began in 2003 and continues to the end of the time series, 2009. This observation for KGSO relates to the decoupling discovered in the deviation statistic for T_(avg-mly-min) and T_(avg-mly-max). The continuing significant difference between T_(avg-mly-min) and T_(avg-mly-max) at KGSO will have lasting influences on local climate records. KGSO serves as the primary climate observation for the Piedmont Triad urban region. This will alter long-term averages as well as give temperature readings not representative of the region.

Different correlations were observed for all three weather stations. The July T_(avg-mly-min) and the three-month period T_(avg-mly-min) for KGSO showed positive correlations with commercial/industrial development. The July T_(avg-mly-max) and the three-month period T_(avg-mly-max) for KGSO showed no correlation. This is consistent with a UHI effect. i.e., minimum temperature responds to increased impervious surface, but maximum temperature does not. The correlation detected at KGSO was not seen at KCLT or KRDU.

Future Use of Site Suitability Model for Weather Observations Impacted by an UHI

The raster data model proved to be applicable for weather station siting after performing post-analysis procedures. The first step was to remove isolated individual cells that passed the raster data model. This was accomplished by converting the raster data output to vector data through a GIS conversion tool. A selection by attributes was performed to find sites ≥ 1 hectare as defined by the WMO (WMO, 2004). The next step involved analyzing these selected sites for openness and flatness. This involved creating buffers around center points of passing sites to measure how close obstructions were to passing sites. The most recent orthoimagery (2010 North Carolina State Orthoimage) was used to find obstructions within the buffers. The fewer the obstructions inside these buffers, the more open the site was deemed to be. This narrowed the search from ten possible sites to six. The six remaining sites were visited in person to further confirm the validity of the raster data model.

First, openness was double checked. It is possible with older spatial data to have new construction, ponds, tree lines, or other objects present at the surface but not observed in the data used to create the model. Second, vegetation was analyzed at the surface. Sites with understory trees and shrubs or tall crops such as corn can impact the ability of the air to mix near the surface. Third, the slope of the land was observed at each site. Locations with steep slopes could alter wind and mixing. Also, if the site is lower than surrounding land on the periphery then cold air drainage could be a problem. The final observation was to confirm accessibility to the potential site. When a weather station is in need of repair from damage or routine maintenance, it must be accessible.

This study encompassed a broad area of research including: Climatology, GIS, and Urban Planning. The climate findings unambiguously indicated that an UHI is affecting KGSO, which appeared to be related to the commercial/industrial development adjacent to PTIA. The raster data model was applicable and worked well for a first run. Future work would allow one to fine tune the model once newer and higher quality spatial data becomes available. Also, future work could allow for the separation of public vs. private land-use in the model.

The next step should be to test weather instruments at the selected site(s). Data will need to be collected for several years (ideally 30 years) in order to statistically compare the data to KGSO. When sufficient data has been collected, then it can be tested to find the 'climatic compatibility' to KGSO prior to the onset of the UHI effect.

Other steps or directions this research can take would be to apply this model to other ASOS sites impacted by a known UHI effect. Reducing microclimate effects in climate records can help improve meteorological and climatological forecasting.

The vast growth in industrial and commercial development around PTIA has had a negative impact on climate; however, it has had a positive economic outcome. New industry and development creates jobs for individuals in the area. It is smart to place this zoning in close proximity to the airport and along major interstate highways. This allows for efficient transportation of freight, but also keeps other uses such as neighborhoods, schools, churches, etc. away from Airport Hazard Zones. Planners should create tighter restrictions on commercial and industrial land-use to off-set the formation of an urban heat island. This includes higher albedo building materials, vegetation, and shading.

Further research on urban heat islands contaminating local climate data will need to be considered. ASOS weather stations impacted by an UHI will produce Climate Normals representative of toposcale climate. The function of an ASOS weather station is to measure synoptic-scale weather phenomenon for the region. As a result, first and last frost/freeze dates will be impacted. This is very important, especially for agriculture. Other impacts include higher cooling costs inside urban areas and poor air quality.

REFERENCES

(2006). Chapter 1 — General. *Guide to Meteorological Instruments and Methods of Observation* (pp. I.1-1-I.1-22). Geneva, Switzerland: Secretariat of the World Meteorological Organization.

(2004, October 16). The State-of-the-Art of Instruments and Automated Surface Observing Systems (ASOS): Development of Siting Criteria and Metadata Standards. Retrieved from World Meteorological Organization website: http://www.wmo.int/pages/index_en.html

(2011). Raster Data Model. Retrieved from ESRI website: http://support.esri.com/en/knowledgebase/GISDictionary/term/raster%20data%20model

(2011, January 19). Cooperative Stations. website: http://www.ncdc.noaa.gov/oa/climate/stationlocator.html

Atkinsin, B. W. (2003). Numerical Modelling of Urban Heat-Island Intensity. *Boundary-Layer Meteorology*, *109*, 285-310.

Baik, J., Kim, Y., Kim, J., & Han, J. (2007). Effects of boundary-layer stability on urban heat island-induced circulation. *Theoretical and Applied Climatology*, *89*, 73-81.

Bejaran, R. A., & Camilloni, I. A. (2003). Objective method for classifying air masses: An application to the analysis of Buenos Aires' (Argentina) urban heat island intensity. *Theoretical and Applied Climatology*, *74*, 93-103.

Coutts, A., Beringer, J., & Tapper, N. (2010). Changing Urban Climate and CO2 Emissions: Implications for the Development of Policies for Sustainable Cities. *Urban Policy and Research*, 27-47.

Chang, C.-, Li, M.-, & Chang, S.- (2007). A preliminary study on the local cool-island intensity of Taipei city parks. *Landscape and Urban Planning*, 386-395.

Easterling, D. R., Horton, B., Jones, P. D., Peterson, T. C., Karl, T. R., Parker, D. E., . . . Folland, C. K. (1997). Maximum and minimum temperature trends for the globe. *SCIENCE*, *277*, 364-367.

Fast, J. D., Torcolini, J. C., & Redman, R. (2005). Pseudovertical Temperature Profiles and the Urban Heat Island Measured by a Temperature Datalogger Network in Phoenix, Arizona. *Journal of Applied Meteorology*, *44*, 3-13.

Gober, P., Brazel, A., Quay, R., Mint, S., Grossman-Clarke, S., Miller, A. , & Rossi, S. (2010). Using Watered Landscapes to Manipulate Urban Heat Island Effects. *Journal of the American Planning Association*, 109-121.

Han, J., & Baik, J. (2008). A Theoretical and Numerical Study of Urban Heat Island-Induced Circulation and Convection. *Journal of Atmospheric Sciences*, *June*, 1859-1877.

Hawkins, T. W., Brazel, A. J., Stefanov, W. L., Bigler, W., & Saffell, E. M. (2004). The role of rural variability in urban heat island determination for Phoenix, Arizona. *Journal of Applied Meteorology*, *43*, 476-486.

Kar, B., & Hodgson, M. E. (2008). A gis-based model to determine site suitability of emergency evacuation shelters. *Transactions in GIS*, *12*(2), 227-248.

Khaikine, M. N., Kuznetsova, I. N., Kadygrov, E. N., & Miller, E. A. (2006). Investigation of temporal-spatial parameters of an urban heat island on the basis of passive microwave remote sensing. *Theoretical and Applied Climatology*, *84*, 161-169.

Khan, S. M., & Simpson, R. W. (2001). Effect of a heat island on the meteorology of a complex urban airshed. *Boundary-Layer Meteorology*, *100*, 487-506.

King'uyu, S. M., Ogallo, L. A., & Anyamba, E. K. (2000). Recent trends of minimum and maximum surface temperatures over eastern Africa. *Journal of Climate a T E, 13*, 2876-2886.

Kolokotsa, D., Psomas, A., & Karapidakis, E. (2009). Urban heat island in southern Europe: The case study of Hania, Crete. *Solar Energy*, *83*, 1871-1883.

Lee, S., & French, S. P. (2009). Regional impervious surface estimation: An urban heat island application. *Journal of Environmental Planning and Management*, *52*(4), 477-496.

Memon, R. A., Leung, D. Y., & Liu, C. (2009). An investigation of urban heat island intensity (UHII) as an indicator of urban heating. *Atmospheric Research*, *94*, 491-500.

Nakayama, T., & Fujita, T. (2010). Cooling effect of water-holding pavements made of new materials on water and heat budgets in urban areas. *Landscape and Urban Planning*, 57-67.

Nichol, J. E., Fung, W. Y., Lam, K., & Wong, M. S. (2009). Urban heat island diagnosis using ASTER satellite images and 'in situ' air temperature. *Atmospheric Research*, *94*, 276-284.

Niino, H., Mori, A., Satomura, T., & Akiba, S. (2006). Flow Regimes of Nonlinear Heat Island Circulation. *Journal of the Atmospheric Sciences*, *63*, 1538-1547.

Sarrat, C., Lemonsu, A., Masson, V., & Guedalia, D. (2006). Impact of urban heat island on regional atmospheric pollution. *Atmospheric Environment*, *40*, 1743-1758.

Smith, C., & Levermore, G. (2008). Designing urban spaces and buildings to improve sustainability and quality of life in a warmer world. *Energy Policy*, 4558-4562.

Stone, B., & Norman, J. M. (2006). Land use planning and surface heat island formation: A parcel-based radiation flux approach. *Atmospheric Environment*, 3561-3573.

Synnefa, A., Dandou, A., Santamouris, M., & Tombrou, M. (2008). On the Use of Cool Materials as a Heat Island Mitigation Strategy. *Journal of Applied Meteorology & Climatology*, 2846-2856.

Taha, H. (2008). Meso-urban meteorological and photochemical modeling of heat island mitigation. *Atmospheric Environment*, *42*, 8795-8809.

Takebayashi, H., & Moriyama, M. (2009). Study on the urban heat island mitigation effect achieved by converting to grass-covered parking. *Solar Energy*, 1211-1223.

Yang, F., Lau, S. S., & Qian, F. (2011). Urban design to lower summertime outdoor temperatures: An empirical study on high-rise housing in Shanghai. *Building and Environment*, 769-785.

Young-bae, S. (2005). Influence of new town development on the urban heat island – The case of the Bundang area. *Journal of Environmental Sciences*, 641-645.

Zhang, H., Sato, N., Izumi, T., Aramaki, T., & Hanaki, K. (2008). Modified RAMS-Urban Canopy Model for Heat Island Simulation in Chongqing, China. *Journal of Applied Meteorology & Climatology*, *47*, 509-524.

APPENDIX A

CLIMATE NORMALS FOR KGSO

GSO 1981 - 2010 Climate Normals

	Jan	Feb	Mar	Apr	May	June	Jul	Aug	Sept	Oct	Nov	Dec	*Ann.*
Max	48.3	52.5	60.9	70.2	77.5	84.8	87.9	86.3	79.7	70.3	60.8	50.7	69.2
Min	29.5	32.4	39.1	47.3	56.1	65.3	69.1	68.0	60.6	48.8	39.6	32.0	49.0

GSO 1971 - 2000 Climate Normals

	Jan	Feb	Mar	Apr	May	June	July	Aug	Sept	Oct	Nov	Dec	*Ann.*
Max	47.2	51.7	60.3	69.7	76.9	83.8	87.6	85.7	79.4	69.6	59.9	50.6	68.5
Min	28.2	30.6	37.8	45.5	54.7	63.5	68.1	66.8	60.1	47.5	38.6	31.4	47.7

Diff Max	1.1	0.8	0.6	0.5	0.6	1.0	0.3	0.6	0.3	0.7	0.9	0.1	0.6
Diff Min	1.3	1.8	1.3	1.8	1.4	1.8	1.0	1.2	0.5	1.3	1.0	0.6	1.3

Source: National Climatic Data Center

APPENDIX B

JUNE RECORDS FOR KGSO

Day	High	Year	High Min	Year	High Min	Year ≥ 1990
1	95	1937	72	1991	72	1991
2	100	1951	71	2011	71	2011
3	98	1951	71	1951		
4	96	1943	71	1981		
5	96	1943	73	2008	73	2008
6	96	1943	73	1981		
7	94	1952	73	2008	73	2008
8	98	1933	73	2008	73	2008
9	99	1933	72	2007	72	2007
10	97	1947	75	1981		
11	95	1947	74	1981		
12	95	1944	72	1998	72	1998
13	96	1945	73	2005	73	2005
14	94	1964	71	1945		
15	95	1981	73	1981		
16	95	1957	73	2004	73	2004
17	98	1944	76	2004	76	2004
18	100	1944	73	1970		
19	100	1944	77	1970		
20	99	1933	75	2008	75	2008
21	100	1933	73	1990	73	1990
22	99	1933	75	1981		
23	97	1988	73	2010	73	2010
24	100	1930	74	2010	74	2010
25	99	1952	74	2010	74	2010
26	101	1952	74	2010	74	2010
27	102	1954	76	1969		
28	99	1959	76	1969		
29	99	1959	74	1969		
30	101	1959	74	1936		

Source: National Climatic Data Center

APPENDIX C

JULY RECORDS FOR KGSO

Day	High	Year	High Min	Year	High Min	Year ≥ 1990
1	98	1954	77	1970		
2	98	1954	74	1970		
3	97	1970	73	1941		
4	98	1970	72	2005	72	2005
5	98	1990	74	1999	74	1999
6	100	1977	76	1999	76	1999
7	101	1977	73	2004	73	2004
8	102	1977	76	2010	76	2010
9	101	1993	76	1987		
10	99	1990	77	1981		
11	98	1990	75	1992	75	1992
12	98	1930	76	2005	76	2005
13	98	1954	75	1981		
14	102	1954	77	1981		
15	97	1974	73	1992	73	1992
16	98	1980	75	2010	75	2010
17	97	1980	73	2005	73	2005
18	97	1986	76	1986		
19	98	1977	74	1996	74	1996
20	100	1977	75	1986		
21	99	1983	76	2011	76	2011
22	100	1952	76	2010	76	2010
23	99	1952	78	2010	78	2010
24	96	1995	78	2010	78	2010
25	97	1987	78	2010	78	2010
26	98	2005	75	2010	75	2010
27	99	1940	76	2005	76	2005
28	100	1952	74	1987		
29	101	1952	75	1993	75	1993
30	97	1954	74	1931		
31	98	1953	74	2006	74	2006

Source: National Climatic Data Center

APPENDIX D

AUGUST RECORDS FOR KGSO

Day	High	Year	High Min	Year	High Min	Year ≥ 1990
1	97	1970	75	2006	75	2006
2	99	1953	76	2006	76	2006
3	98	1942	76	2006	76	2006
4	98	1987	76	2006	76	2006
5	101	1930	76	2006	76	2006
6	98	2007	75	2007	75	2007
7	99	1977	77	2007	77	2007
8	100	2007	77	2007	77	2007
9	101	2007	80	2007	80	2007
10	100	2007	76	2007	76	2007
11	95	1983	75	2007	75	2007
12	96	1995	73	1980		
13	97	1995	74	1995	74	1995
14	99	1995	75	1995	75	1995
15	98	2007	77	1995	77	1995
16	99	2007	75	2007	75	2007
17	99	1988	75	2010	75	2010
18	103	1988	75	1995	75	1995
19	99	1988	76	1969		
20	100	1983	75	2007	75	2007
21	100	2007	75	1968		
22	100	1983	74	2006	74	2006
23	99	1983	73	2007	73	2007
24	98	1968	73	2007	73	2007
25	97	2007	75	2007	75	2007
26	98	1975	73	1975		
27	96	1987	75	1998	75	1998
28	98	1948	73	2003	73	2003
29	100	1948	74	2003	74	2003
30	100	1932	73	2005	73	2005
31	101	1932	72	2005	72	2005

Source: National Climatic Data Center

APPENDIX E

METAR REPORTS

METAR KGSO 091054Z 00000KT 5SM HZ FEW110 27/21 A2994 RMK AO2 SLP125 T02720206

METAR KCLT 091052Z 33004KT 7SM FEW140 26/21 A2994 RMK AO2 SLP129 T02560211

METAR KRDU 091051Z 00000KT 5SM BR FEW100 SCT150 BKN200 26/23 A2990 RMK AO2 SLP119 T02560233

Source: National Climatic Data Center

Decode a METAR weather report: http://www.nws.noaa.gov/oso/oso1/oso12/document/guide.shtml

APPENDIX F

WMO SITE CRITERIA

1.3.3.1 SITE SELECTION

Meteorological observing stations are designed to enable representative measurements (or observations) to be made according to the type of station involved. Thus, a station in the synoptic network should make observations to meet synoptic-scale requirements whereas an aviation meteorological observing station should make observations that describe the conditions specific to the local (aerodrome) site. Where stations are used for several purposes, e.g. aviation, synoptic and climatology, the most stringent requirement will dictate the precise location of an observing site and its associated sensors. A detailed study on siting and exposure is published by WMO (1993*a*).

As an example, the following considerations apply to the selection of site and instrument

1. Outdoor instruments should be installed on a level piece of ground
2. There should be no steeply sloping ground in the vicinity and the site should not be in a hollow.
3. The site should be well away from trees, buildings, walls or other obstructions. The distance of any such obstacle(including fencing) from the raingauge should not be less than twice the height of the object above the rim of the gauge, and preferably four times the height;

Source: World Meteorological Organization

APPENDIX G

JANUARY RECORDS FOR KGSO

Day	High	Year	High Min	Year	High Min	Year ≥ 1990
1	75	1985	54	1966		
2	76	1952	58	1966		
3	72	2004	54	1950		
4	74	2005	57	1950		
5	71	1950	57	2007	57	2007
6	70	1955	58	1950		
7	71	1982	61	1998	61	1998
8	68	1998	60	1998	60	1998
9	70	2003	55	1937		
10	73	1949	58	1937		
11	67	2000	51	1972		
12	67	2005	53	1963		
13	73	1960	61	1932		
14	71	2007	59	1995	59	1995
15	73	1960	59	1932		
16	71	1953	53	1947		
17	76	1943	63	1943		
18	66	1937	60	1943		
19	67	1951	50	1933		
20	70	1951	50	1954		
21	72	1933	54	1954		
22	72	1967	59	1933		
23	73	1967	57	1999	57	1999
24	76	1967	52	2002	52	2002
25	75	1950	57	1950		
26	74	1950	59	1950		
27	72	1974	55	1952		
28	78	1944	54	1944		
29	78	1975	55	1957		
30	78	2002	56	1947		
31	74	1975	56	2002	56	2002

Source: National Climatic Data Center